

Article

Effects of Atmospheric Dry Deposition on External Nitrogen Supply and New Production in the Northern South China Sea

Hung-Yu Chen ^{1,2,*}  and Shih-Zhe Huang ¹

¹ Department of Marine Environmental Informatics, National Taiwan Ocean University, Keelung 202, Taiwan; benson50705@gmail.com

² Center of Excellence for the Oceans, National Taiwan Ocean University, Keelung 202, Taiwan

* Correspondence: hychen@mail.ntou.edu.tw

Received: 27 August 2018; Accepted: 1 October 2018; Published: 3 October 2018



Abstract: The South China Sea (SCS) is one of the world's largest oligotrophic marginal seas. Increases in biomass and primary production in the surface layer of the northern SCS are affected by anthropogenic aerosol use among north Asian peoples. The seasonal variation of dry deposition and its contribution to new production in the ocean are vital to determining the effect that such dry deposition has on the biogeochemical cycle of the SCS. This study collected 240 samples of total suspended particles at Dongsha Island in the northern SCS from April 2007 to March 2009; the major ions and water-soluble nitrogen species in the samples were analyzed. The analysis results indicated that the concentration distributions of major water-soluble ions and nitrogen species in total suspended particles exhibited significant seasonal (source) variation. The north-east monsoon seasons (autumn to spring) brought relatively high concentrations because most air masses during this period arrived from the northern continental region. We found that the concentration of nitrogen species shows a latitude distribution, gradually decreasing from north to south. In addition, this study also discovered that the ratio of organic nitrogen to total dissolved or water-soluble nitrogen also varies in a similar manner, resulting in a concentration of <20% for locations north of 30° N and >30% for those south of 30° N. Aerosols at Dongsha Island mainly comprised sea salt; however, significant chloride depletion was observed during the north-east monsoon season. The molar ratio of NH_4^+ to non-sea salt (NSS) sulfate (nss-SO_4^{2-}) was 0.8, indicating that the amount of artificially produced NH_4^+ in the region was insufficient for reaction with nss-SO_4^{2-} . Therefore, NH_4^+ was mainly present in the form of NH_4HSO_4 . The fluxes of water-soluble inorganic nitrogen (WSIN) and water-soluble organic nitrogen (WSON) within the region were 23 ± 13 and 27 ± 15 $\text{mmol m}^{-2} \text{y}^{-1}$, respectively. The new production converted from atmospheric water-soluble nitrogen species in the northern SCS was estimated to be 0.52–0.81 $\text{mmol C m}^{-2} \text{d}^{-1}$. This flux made about 5.6–8.7% (the global average was about 3.5%) contribution to the primary production (9.24 $\text{mmol C m}^{-2} \text{d}^{-1}$) of the SCS surface water. This result indicates that the ocean's external nitrogen supply, provided by anthropogenic aerosols, is vital for the biogeochemical cycle in Asian marginal seas, particularly the northern SCS.

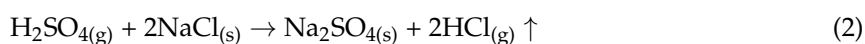
Keywords: South China Sea; ocean's external nitrogen supply; water-soluble inorganic nitrogen; water-soluble organic nitrogen; new production

1. Introduction

Anthropogenic and natural sources of aerosols have a substantial effect on global weather and atmospheric chemistry, and they have a particular influence on the marine ecosystem in the pelagic zone [1]. North-east Asia has experienced rapid development of economic and agricultural

activities; the use of vast quantities of fossil fuels and fertilizers has resulted in a significant increase in anthropogenic gas emissions and particulates [2]. In addition, high concentrations of dust and anthropogenic aerosols produced in the springtime in continental Asia are transmitted to the North Pacific region by monsoon systems. Occasionally, these concentrations might even be transmitted to North America on westerly winds, affecting the global radiation balance and atmospheric chemistry as well as the biogeochemical cycle [3].

Generated by the effect of wind on the ocean's surface, sea salt aerosols are one of the major components of the total aerosol mass near the Earth's surface. The major ions they contain are similar to those in seawater, with chloride ions contributing to the majority of aerosol mass and concentration [4]. Na^+ , Mg^{2+} , and Cl^- in the atmosphere mostly originate from sea spray and are either swiftly deposited on land or returned to the ocean. High concentrations of Na^+ and Cl^- are common in aerosols near the coast. During the deposition process, sea salt aerosols not only react with acidic compounds to form volatile hydrogen chloride gas, which quickly vaporizes, but also absorb non-sea salt (NSS) ions (e.g., NH_4^+ and NSS-SO_4^{2-}) during atmospheric transmission [5]. This reaction, which leads to a decrease in the Cl^- concentration in aerosols, is known as chloride depletion and proceeds as follows:



The level of chloride depletion is calculated as follows [6]:

$$\text{Cl}^- \text{ depletion } (\%) = (1.17 \times [\text{Na}^+]_{\text{measured}} - [\text{Cl}^-]_{\text{measured}}) / 1.17 \times [\text{Na}^+]_{\text{measured}} \times 100\% \quad (3)$$

where 1.17 is the molar concentration of Cl^- and Na^+ in seawater and $[\text{Na}^+]_{\text{measured}}$ and $[\text{Cl}^-]_{\text{measured}}$ are the concentrations of Cl^- and Na^+ (nmol m^{-3}) in the aerosol, respectively.

Hsu et al. noted that chloride depletion from aerosols occurs at a high level in the South China Sea (SCS), reaching 30% for coarse particle aerosols and up to 85% for fine particle aerosols [7]. The level of chloride depletion from sea salt aerosols often depends on particle size; for example, the degree of chloride depletion in aerosols comprising coarse particles decreases with particle size. However, for fine particles, the degree of chloride depletion is strongly affected by particle size enrichment of SO_4^{2-} . This phenomenon is also apparent in aerosols situated around coastal areas and in the pelagic zone [8].

The world's population has increased by 78% since 1970, causing a concurrent increase in energy use and food demand that has raised the level of reactive nitrogen (Nr) by 120% [9]. In 2010, 75% of Nr on land was created through anthropogenic activities (210 Tg N y^{-1}), which was three times higher than that from natural continental sources (63 Tg N y^{-1}). Contributions from natural marine sources (140 Tg N y^{-1}) also play a vital role in the global nitrogen cycle [10]. In 2010, China was the world's largest source of NH_3 emissions ($\sim 15 \text{ Tg NH}_3\text{-N y}^{-1}$), most of which were products of animal husbandry and agricultural fertilizer use [11,12]. Wu et al. stated that NH_3 plays an essential role in severe haze events, and that it is also a key factor in the formation of secondary aerosols in urban areas, of which secondary inorganic aerosols, such as ammonium sulfate ($(\text{NH}_4)_2\text{SO}_4$) and ammonium nitrate (NH_4NO_3), are the most representative [13]. Through molecular dynamics simulation, Li et al. revealed that ammonium bisulfate (NH_4HSO_4), which is formed on the surface of water droplets from NH_3 and SO_3 hydrates, is the main precursor for the formation of ammonium sulfate [14]. Zhu et al. noted that most NH_4^+ and SO_4^{2-} in aerosols are enriched in fine particles. NH_4^+ first neutralizes with SO_4^{2-} , which generates $(\text{NH}_4)_2\text{SO}_4$ when the molar ratio is >2 and NH_4HSO_4 when the molar ratio is <2 . When the molar ratio is <2 , the atmosphere contains relatively low NH_4^+ content, which cannot completely neutralize with SO_4^{2-} , thus producing NH_4HSO_4 [15].

In 1860, the Nr deposition in most sea areas worldwide was $<50 \text{ mg N m}^{-2} \text{ y}^{-1}$ and was $>200 \text{ mg N m}^{-2} \text{ y}^{-1}$ in a few areas. At that time, most oceanic deposition originated from natural

sources, with anthropogenic sources only affecting a few coastal areas. Following industrialization and the development of intensive farming, N_r deposition was affected by the strong deposition effect of westward winds from areas with high population density, including Asia, India, the United States, Europe, and West Africa in 2000 [16]. N_r deposition in most sea areas had reached $200 \text{ mg N m}^{-2} \text{ y}^{-1}$, with some regions even reaching $> 700 \text{ mg N m}^{-2} \text{ y}^{-1}$. N_r from anthropogenic sources provides approximately one-third of the ocean's external nitrogen supply, with an annual 3% ($\sim 0.3 \text{ Pg C y}^{-1}$) new production in the ocean [17]. Chen et al. noted that the water-soluble total nitrogen (WSTN) from aerosols in the southern East China Sea was $4.86 \text{ g C m}^{-3} \text{ y}^{-1}$, contributing to 8.2% of the new production of seawater, where the contribution rate of inorganic to organic nitrogen was 64:36 [17]. These results reveal the vital role that water-soluble nitrogen species in atmospheric aerosols play in the nutrient biogeochemical cycle of marginal seas in East Asia [18]. Inorganic nitrogen is easily utilized by marine organisms, whereas organic nitrogen can only be partially utilized. The bioavailability of organic nitrogen in the atmosphere is mainly determined by the atmosphere's chemical composition. Most organic nitrogen substances, such as amino acids, urea, and amines, can be processed by marine microorganisms within a short amount of time; however, humic-like substances are too difficult for such organisms to use [19].

The SCS is located between the tropics and subtropics, and it is the largest marginal sea (approximately $3.5 \times 10^6 \text{ km}^2$) of the north-western Pacific Ocean [20]. The SCS is surrounded by densely populated regions undergoing rapid economic growth, including China, Taiwan, the Philippines, the Malay Archipelago, and the Indochinese Peninsula. These regions are responsible for emissions of large amounts of anthropogenic aerosols, which are deposited into the SCS through rivers and the atmosphere. In the next few decades, the amount of N_r deposition caused by anthropogenic activities in the SCS is estimated to exceed that in all other marginal seas combined [16]. The SCS is affected by the East Asian monsoon system, with a strong north-east monsoon in the winter and spring, and a south-west monsoon in the summer [21]. Hsu et al. found that dust and large amounts of pollutants transported from deserts and arid regions in northern China were detected in the SCS and coastal areas during the winter monsoon [7]. Compared with adjacent marginal seas (i.e., the East China Sea and Yellow Sea), the marine productivity of the SCS is relatively low, and large amounts of atmospheric nitrogen input have caused the SCS to be more susceptible to the effects of anthropogenic nitrogen deposition. Therefore, the SCS has become a key area for studying the effect of anthropogenic nitrogen deposition on marine productivity.

Based on estimates from satellite data, Kim et al. calculated the input flux of atmospheric N_r (including organic and inorganic nitrogen) in the SCS to be approximately $55 \text{ mmol N m}^{-2} \text{ y}^{-1}$ [22], which in turn increased the new production of surface seawater to $50\text{--}80 \text{ mg C m}^{-2} \text{ d}^{-1}$. This flux contributes to approximately 20% of new surface seawater production in the oligotrophic waters of the SCS, indicating that atmospheric nitrogen deposition is a crucial external source for the SCS area. Calculated accordingly, the total nitrogen flux for the entire SCS can reach approximately 77 Gmol N y^{-1} . The Mekong and Pearl Rivers in this region discharge 20 and 26 Gmol N y^{-1} , respectively, to the SCS [23,24], causing the flux of the rivers to be less than the atmospheric flux. Thus, the nitrogen input of coastal rivers to the ocean may be less than that of the atmosphere [25].

Having established a preliminary scientific understanding of the biogeochemical cycle of nitrogen, research is increasingly focusing on the effect of atmospheric nitrogen deposition in seas across the globe. Currently, knowledge regarding the temporal variation and chemical composition of water-soluble nitrogen species and major ions in the SCS region remains limited. Therefore, this study undertook long-term monitoring of major ions and water-soluble nitrogen species in the dry deposition of atmospheric suspended particles in the northern SCS (i.e., Dongsha Island) to explore their seasonal variation, composition, distribution, and source. In addition, the flux of nitrogen species was estimated for comparison with data regarding nitrogen species in dry deposition in East Asia to determine regional variation. To investigate the impact of atmospheric nitrogen species on the nitrogen cycle in surface seawater, the present study also examined the effect of dry deposition on the biogeochemistry

of the northern SCS as well as new production induced by atmospheric nitrogen deposition in the surface seawater of marginal seas in East Asia.

2. Methodology

2.1. Sampling

Dongsha Island is a reef island in the northern SCS (Figure 1), located approximately 400 km away from Taiwan's main island, 340 km from Hong Kong, and 780 km from Manila in the Philippines. Dongsha Island is west–north–west/east–south–east aligned, with a land area of 1.74 km². The sampling station, 6 m above ground, was located in the attic of the Dongsha Island weather station (20°42' N, 116°43' E). Compiled by the Naval Meteorological and Oceanographic Office, the meteorological data used for this study included temperature, wind speed, wind direction, precipitation, relative humidity, and precipitation days. From April 2007 to March 2009, a high volume collector (GS2313-105; Thermo Fisher Scientific Inc, Franklin, MA, USA) and quartz filter paper (QR-100, 254 × 203 mm²; Advantec Group, Toyo, Japan) were used to collect samples of atmospheric total suspended particle (TSP). A total of 240 sets of samples were collected, with a flow rate of 1.3 m³ min⁻¹, and the collection time for each sample set was approximately 24 h. Each sampled filter paper was wrapped in aluminum foil and stored in a freezer at -24 °C. The filter paper was lyophilized in a freeze dryer for 72 h to remove its moisture. Finally, the filter paper was divided into two equal segments using a cutter and placed in a zipper bag to be sealed and stored in a freezer at -24 °C for subsequent analysis.

2.2. Chemical Analysis

One-half of the filter paper was removed from the freezer and placed in a brown wide-mouth bottle, into which 250 mL of deionized water (>18 MΩ cm⁻¹, RDI-20; Lotuntech, Taipei, Taiwan) was added. The bottle was then shaken using an ultrasonic oscillator for 3 h for extraction [17,26]. Because an excessively high water temperature caused by over-oscillation might affect the chemicals in the bottle, the water was replaced every hour to reduce the temperature. The obtained extract was filtered through a quartz filter paper (0.8 μm, 25 mm; Advantec Group, Toyo, Japan) to acquire clarified liquid for analysis.

An ion chromatography system (ICS-1000; Dionex, Sunnyvale, CA, USA) was used to analyze the major anions (Cl⁻ and SO₄²⁻) and cations (Na⁺, K⁺, Mg²⁺, and Ca²⁺). For the anions, AS4A-SC (Dionex, Sunnyvale, CA, USA) was used as the chromatography column, AG4A-SC as the guard column, and a mixed solution of Na₂CO₃ and NaHCO₃ as the eluent. For the cations, CS12A (Dionex, Sunnyvale, CA, USA) was used as the chromatography column, CG12A as the guard column, and methanesulfonic acid as the eluent. The experimental procedure was the same as that detailed in [18].

To determine the water-soluble inorganic nitrogen (WSIN) species concentration, the indophenol blue colorimetric method was employed for NH₄⁺ [27] and the pink azo compound colorimetric method for NO₂⁻ [28]. For NO₃⁻ analysis, the extract was first passed through a copper-cadmium reduction column, and it was then reduced to nitrite and assessed using the pink azo compound colorimetric method. Finally, the concentration of NO₃⁻ was obtained after deducting the NO₂⁻ concentration in the sample [29]. Water-soluble total nitrogen (WSTN) was analyzed by adding persulfate oxidizing (PO) agent to the sample, which was then placed in an ultraviolet (UV) chamber for 24 h [30], causing the water-soluble organic nitrogen (WSON) to oxidize with the other nitrogen species to form NO₃⁻. Determined through the cadmium-copper reduction method, the concentration of total inorganic nitrogen in the sample indicated the concentration of total nitrogen. Urea, quinolone, and ethylenediaminetetraacetic acid (EDTA) were employed to determine the oxidation efficiency of WSTN, ensuring that the recovery rate was within an acceptable range. The obtained oxidation efficiency result is similar to that acquired by [18], as shown in Table 1.

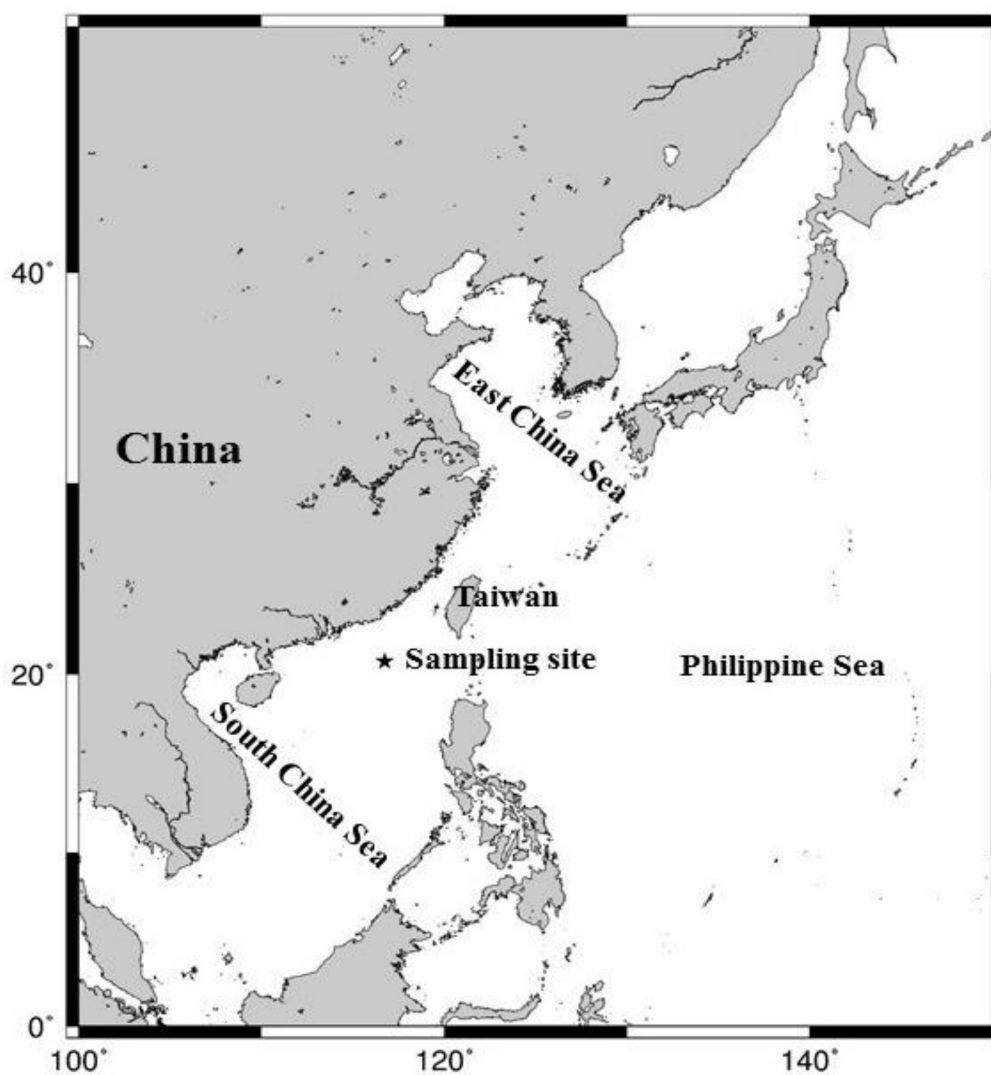


Figure 1. The location of the sampling site.

Table 1. Recovery of organic nitrogen species using ultraviolet (UV) + persulfate oxidizing (PO) methods.

	Recovery (%)		
	This Study (<i>n</i> = 10)	Chen et al. [18] (<i>n</i> = 8)	Bronk et al. [30] (<i>n</i> = 5)
Antipyrine			68 ± 6
EDTA	99 ± 5	92 ± 3	94 ± 2
Quinoline	92 ± 15	94 ± 4	
Urea	102 ± 7	94 ± 5	92 ± 9

WSIN contains ammonium, nitrite, and nitrate. In the present study, the concentration of WSTN minus that of WSIN equaled the WSON concentration of a sample. The concentration of nitrogen species (nmol m^{-3}) was calculated as follows:

$$[\text{WSIN}] = [\text{NH}_4^+] + [\text{NO}_2^-] + [\text{NO}_3^-] \quad (4)$$

$$[\text{WSTN}] = [\text{WSIN}] + [\text{WSON}] \quad (5)$$

The blank test and limit of detection results for anions, cations, ammonium, nitrite, and nitrate are shown in Table 2. All obtained concentrations of aerosol samples were at least three times higher than in the blank measurements.

Table 2. Blank values and limit of detection (LOD) for water-soluble nutrients and ions.

	Blank (nmol m ⁻³)	LOD ^a (nmol m ⁻³)
NH ₄ ⁺	0.09 ± 0.01	0.03
NO ₂ ⁻	0.005 ± 0.002	0.005
NO ₃ ⁻	0.08 ± 0.03	0.08
Na ⁺	0.03 ± 0.01	0.03
K ⁺	0.005 ± 0.002	0.005
Mg ²⁺	0.010 ± 0.003	0.009
Ca ²⁺	0.07 ± 0.02	0.06
Cl ⁻	0.31 ± 0.09	0.26
SO ₄ ²⁻	0.12 ± 0.04	0.12

^a Calculated using 3σ of the blank.

3. Results and Discussion

3.1. Meteorological Characteristics and Air Masses

The meteorological data of Dongsha Island during the research period were as follows: average temperature = 25.9 ± 3.1 °C; average wind speed = 5.2 ± 2.4 m s⁻¹; average relative humidity = 85% ± 3.6%; and average annual accumulated precipitation = 1700 mm. In this study, March–May was considered spring, June–August was summer, September–November was autumn, and December–February was winter. The temperature began to increase in March, reaching the highest average temperature (28–31 °C) between July and September and the lowest (18–20 °C) between January and February. The precipitation and temperature trends were similar, with a wet season in the summer and dry season in the winter. Regarding variation of wind direction, the north-east monsoon was in effect across winter, spring, and autumn, whereas the south-west monsoon occurred in summer; however, the wind direction was prone to drastic changes from June to August because of typhoons. The wind speed was higher in autumn (3.4–8.9 m s⁻¹) and winter (5.4–8.0 m s⁻¹) than it was in spring (3.5–6.7 m s⁻¹) and summer (2.5–3.8 m s⁻¹).

In addition to collecting meteorological data, this study employed the hybrid single-particle Lagrangian integrated trajectory (HYSPLIT) model established by the US National Oceanic and Atmospheric Administration to illustrate air mass back trajectories (AMBTs) for determining the source of air masses during the sampling period. Such trajectories can be used as an auxiliary tool for estimating the source of suspended particles collected in a region. Because the air masses that affected the sampling point were generated approximately 3 days prior to testing, the reversal time in this study was set to 72 h. Referring to the height parameters set by [31], 100, 500, and 1000 m represented the airflow trajectories for estimating the airflow transmission pathway and air mass sources of the research area at low, medium, and high altitudes, respectively. According to the classification method developed by [32], the sources of airflow trajectories during sampling can be divided into three categories according to regional characteristics:

- (1) Northern sources: air masses originating from inland and north-eastern China that are transported by the north-east monsoon.
- (2) Southern sources: air masses originating from the Indochinese Peninsula and SCS that are transported by the south-west monsoon.
- (3) Marine sources: air masses originating from high-pressure areas over the Pacific Ocean that do not pass over land.

Based on the seasons, the backward trajectories of air masses during the study period were statistically analyzed (Table 3). The majority of air masses (157 samples; 65%) recorded on Dongsha Island originated from northern sources. They often developed from autumn and winter, during the north-east monsoon, into the following spring. The other main source of air masses was southern sources (75 samples; 31%), which principally occurred in summer when the southwest monsoon prevailed. A total of 8 (3%) air masses originated from marine sources, primarily during summer.

Table 3. Seasonal statistics of air mass back trajectories (AMBTs).

	North (n = 157)	South (n = 75)	Sea (n = 8)
Spring	82%	15%	3%
Summer	0%	90%	10%
Autumn	83%	17%	0%
Winter	97%	3%	0%

3.2. Concentration of Major Water-Soluble Ions

Major ions are also known as the conservative elements in seawater [33], comprising Na⁺, K⁺, Mg²⁺, Ca²⁺, Cl⁻, and SO₄²⁻. The sources of these ions can be divided into natural and anthropogenic: natural sources include ocean–atmosphere exchange, weathering, and forest fires, whereas anthropogenic sources include substances generated from fossil fuel and biomass combustion as well as emissions from factories and vehicles [34]. Analyzing the relative concentration and composition ratio of ions can determine their sources.

The concentration of sea salt ions during sampling is shown in Table 4 for Na⁺ (23.4–771 nmol m⁻³, average of 280 ± 165 nmol m⁻³); Cl⁻ (16.5–751 nmol m⁻³, average of 240 ± 149 nmol m⁻³); and Mg²⁺ (1.40–80.9 nmol m⁻³, average of 30.2 ± 18.4 nmol m⁻³). Figure 2 shows that temporal variations in the concentration of sea salt ions were similar. November 2007 (winter) was the month with the highest monthly average concentration of Na⁺ (570 ± 173 nmol m⁻³), Cl⁻ (478 ± 155 nmol m⁻³), and Mg²⁺ (63.4 ± 17.0 nmol m⁻³). August 2008 (summer) was the month with the lowest monthly average concentrations of Na⁺ (102 ± 65.9 nmol m⁻³), Cl⁻ (101 ± 76.4 nmol m⁻³), and Mg²⁺ (9.46 ± 7.22 nmol m⁻³). Comparing these findings with the meteorological data reveals that high concentrations of sea salt ions are related to wind speed. This is because the high wind speed of the northeast monsoon creates conditions more conducive to sea spray than the conditions in spring or summer.

Table 4. Monthly average wind speeds (m/s) and concentrations (nmol m⁻³) of major ions and non-sea-salt (NSS) ions in total suspended particle (TSP) samples *.

	Wind Speeds	Na ⁺	Mg ²⁺	Cl ⁻	nss-SO ₄ ²⁻	nss-K ⁺	nss-Ca ²⁺
April 2007	5.1 ± 1.3	343 ± 102	36.0 ± 11.1	281 ± 106	122 ± 85.4	5.45 ± 5.41	8.44 ± 3.74
May 2007	3.6 ± 0.8	211 ± 90.4	24.5 ± 11.4	181 ± 75.2	131 ± 98.0	7.31 ± 5.70	10.7 ± 5.34
June 2007	3.0 ± 0.9	123 ± 57.3	12.2 ± 6.35	136 ± 57.4	18.5 ± 6.25	1.05 ± 0.47	2.70 ± 0.75
July 2007	3.3 ± 0.7	123 ± 73.2	12.2 ± 7.69	134 ± 76.3	25.0 ± 6.29	1.77 ± 0.60	4.34 ± 1.49
August 2007	3.8 ± 1.7	229 ± 193	24.5 ± 21.8	254 ± 199	23.2 ± 17.6	2.13 ± 1.55	3.68 ± 1.18
September 2007	3.6 ± 1.6	201 ± 162	24.0 ± 18.3	170 ± 148	155 ± 155	13.4 ± 14.6	9.12 ± 7.75
October 2007	6.3 ± 1.3	414 ± 148	47.7 ± 16.6	356 ± 150	140 ± 76.1	7.93 ± 7.42	9.21 ± 3.78
November 2007	8.9 ± 1.4	570 ± 173	63.4 ± 17.0	478 ± 155	136 ± 37.1	9.69 ± 3.16	13.1 ± 2.72
December 2007	6.6 ± 1.8	344 ± 96.2	35.2 ± 12.0	235 ± 74.9	170 ± 73.4	12.3 ± 5.97	11.7 ± 6.67
January 2008	6.4 ± 2.5	381 ± 105	36.6 ± 11.8	317 ± 113	83.2 ± 45.8	3.88 ± 3.80	6.38 ± 4.82
February 2008	7.5 ± 1.1	330 ± 101	36.2 ± 10.2	232 ± 109	203 ± 45.1	14.9 ± 6.36	9.59 ± 4.59
March 2008	5.3 ± 1.3	295 ± 94.7	34.0 ± 8.12	201 ± 91.5	160 ± 52.1	11.3 ± 5.30	12.2 ± 5.19
April 2008	3.5 ± 1.3	205 ± 108	21.3 ± 11.9	156 ± 78.3	90.7 ± 29.7	5.66 ± 2.14	8.36 ± 3.19
May 2008	3.6 ± 2.0	220 ± 169	24.3 ± 18.6	158 ± 116	116 ± 66.6	6.85 ± 2.92	9.56 ± 4.31
June 2008	3.5 ± 0.9	173 ± 94.2	16.2 ± 8.97	182 ± 114	17.6 ± 7.54	1.84 ± 0.60	5.00 ± 1.73
July 2008	2.9 ± 1.1	146 ± 75.2	13.9 ± 7.31	145 ± 81.7	17.3 ± 8.15	2.70 ± 0.61	4.24 ± 1.50
August 2008	2.5 ± 0.9	102 ± 65.9	9.46 ± 7.22	101 ± 76.4	23.6 ± 12.3	2.34 ± 1.10	4.67 ± 0.89
September 2008	3.4 ± 1.9	149 ± 169	15.7 ± 18.4	128 ± 187	126 ± 130	7.45 ± 6.79	9.57 ± 4.65
October 2008	6.3 ± 2.3	288 ± 82.1	30.4 ± 10.0	242 ± 82.8	111 ± 65.1	7.38 ± 5.98	9.20 ± 3.49

Table 4. Cont.

	Wind Speeds	Na ⁺	Mg ²⁺	Cl ⁻	nss-SO ₄ ²⁻	nss-K ⁺	nss-Ca ²⁺
November 2008	7.5 ± 1.6	393 ± 96.4	41.3 ± 11.2	345 ± 107	66.8 ± 109	5.45 ± 4.14	6.87 ± 2.18
December 2008	7.8 ± 1.6	458 ± 104	50.1 ± 10.9	396 ± 137	109 ± 73.0	11.5 ± 7.80	13.1 ± 4.99
January 2009	8.0 ± 2.0	393 ± 145	42.8 ± 15.5	342 ± 134	76.1 ± 27.5	8.98 ± 4.60	8.64 ± 2.96
February 2009	5.4 ± 2.6	309 ± 151	34.4 ± 16.7	291 ± 166	58.9 ± 25.2	4.73 ± 1.91	7.19 ± 1.26
March 2009	6.7 ± 1.7	333 ± 104	38.4 ± 11.9	306 ± 85.5	69.7 ± 15.8	4.75 ± 1.46	10.6 ± 3.40
Average	5.2 ± 2.4	280 ± 165	30.2 ± 18.4	240 ± 149	93.8 ± 80.6	6.70 ± 6.33	8.26 ± 4.73

* The daily wind speeds and concentrations of major ions and non-sea-salt (nss) ions can be found in Supplementary 1.

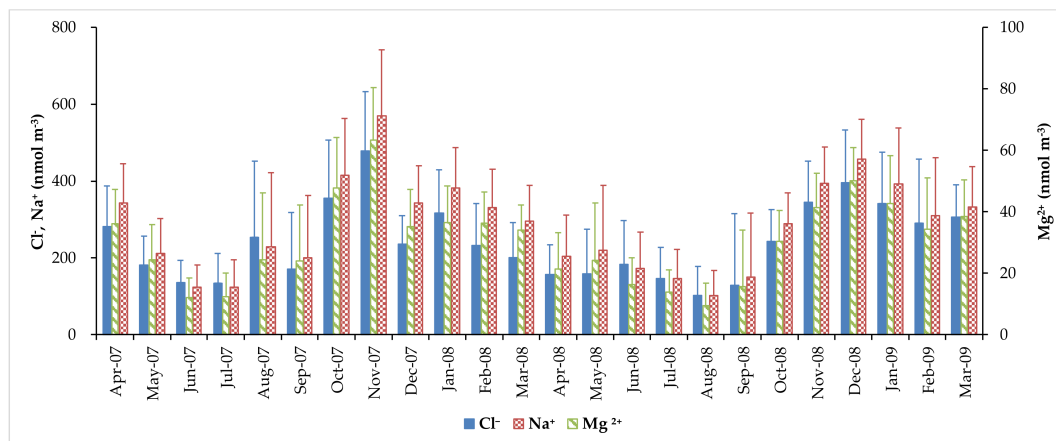
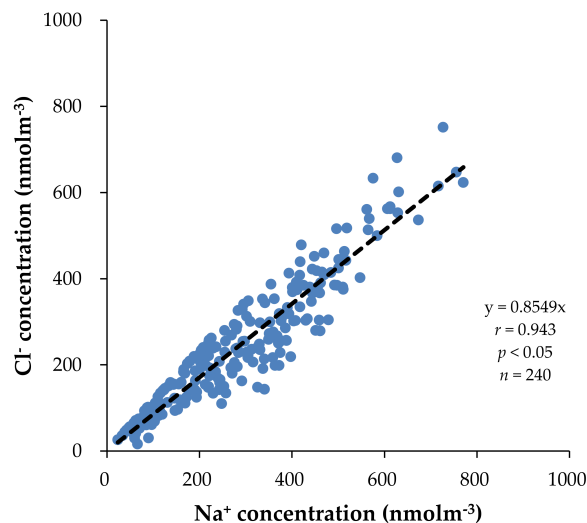


Figure 2. Variations in the monthly average concentrations of sea-salt ions.

A scatter plot of Na⁺ versus sea salt ions (i.e., Cl⁻ and Mg²⁺) is presented in Figure 3, showing a molar concentration ratio Cl⁻/Na⁺ of 0.85 ($r = 0.94; p < 0.05$). That this ratio is significantly lower than that of Cl⁻/Na⁺ in seawater (1.17) suggests that chloride depletion occurred [7]. The annual average chlorine depletion during the study period was 25%. February 2008 (winter) exhibited the highest percentage (42%) of chlorine depletion and August 2007 (summer) the lowest percentage (4.2%). Keen et al. noted that Mg²⁺ is an ideal indicator for marine sources [35]. In this study, the molar concentration ratio Mg²⁺/Na⁺ was 0.11 ($r = 0.99; p < 0.05$), which was consistent with that in seawater. However, the concentration of Mg²⁺ was lower than that of Na⁺. Based on the relative concentrations of Na⁺ and Mg²⁺, Na⁺ can still be regarded as the most suitable indicator for sea salt sources [36].



(a)

Figure 3. Cont.

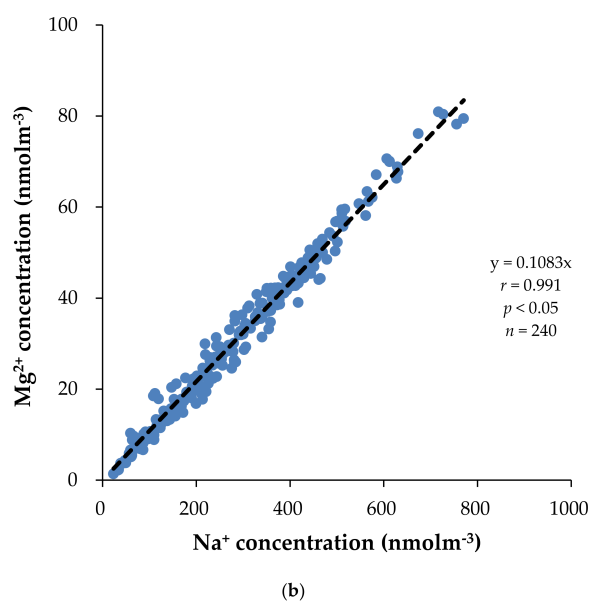


Figure 3. Linear regression diagrams of (a) Cl^- and (b) Mg^{2+} vs. Na^+ .

The molar concentration ratios K^+/Na^+ , $\text{Ca}^{2+}/\text{Na}^+$, and $\text{SO}_4^{2-}/\text{Na}^+$ were 0.04, 0.05, and 0.34, respectively, which were higher than those in seawater (0.02, 0.02, and 0.06, respectively). In addition to sea salt sources, these three ions were inferred to have other sources on Dongsha Island. Chen and Chen subtracted the ratio of these three ions in seawater from their concentration and then defined the obtained values as the concentrations of NSS ions (nmol m^{-3}) [31]; this process was referenced for the following formulas:

$$[\text{nss-K}^+] = [\text{K}^+] - 0.02 \times [\text{Na}^+] \quad (6)$$

$$[\text{nss-Ca}^{2+}] = [\text{Ca}^{2+}] - 0.02 \times [\text{Na}^+] \quad (7)$$

$$[\text{nss-SO}_4^{2-}] = [\text{SO}_4^{2-}] - 0.06 \times [\text{Na}^+] \quad (8)$$

where $[\text{Na}^+]$, $[\text{K}^+]$, $[\text{Ca}^{2+}]$, and $[\text{SO}_4^{2-}]$ are the concentrations of sodium, potassium, calcium, and sulfate ions, respectively, and $[\text{nss-K}^+]$, $[\text{nss-Ca}^{2+}]$, and $[\text{nss-SO}_4^{2-}]$ are the concentrations of NSS potassium, NSS calcium, and NSS sulfate ions, respectively.

In the environment, these NSS ions can be regarded as indicators of different sources: NSS potassium ions (nss-K^+) are mainly derived from biomass combustion and agricultural activities; NSS calcium ions (nss-Ca^{2+}) primarily originate from windblown soil, a crustal source; and NSS sulfate ions (nss-SO_4^{2-}) are mainly generated by anthropogenic activities such as fossil fuel combustion and factory and vehicle emissions [37–39].

The variation in concentration of NSS ions during the sampling period is detailed in Table 4: nss-K^+ ($0.04\text{--}45.6 \text{ nmol m}^{-3}$; average of $6.70 \pm 6.33 \text{ nmol m}^{-3}$); nss-Ca^{2+} ($1.16\text{--}25.6 \text{ nmol m}^{-3}$; average of $8.26 \pm 4.73 \text{ nmol m}^{-3}$); and nss-SO_4^{2-} ($0.27\text{--}437 \text{ nmol m}^{-3}$; an average of $93.8 \pm 80.6 \text{ nmol m}^{-3}$). The trend chart of monthly average concentration of NSS ions (Figure 4) shows that the highest monthly concentration of nss-Ca^{2+} ($13.1 \pm 4.99 \text{ nmol m}^{-3}$) appeared in December 2008 (winter), and the highest monthly concentrations of nss-K^+ ($14.9 \pm 6.36 \text{ nmol m}^{-3}$) and nss-SO_4^{2-} ($203 \pm 45.1 \text{ nmol m}^{-3}$) were in February 2008 (spring). By contrast, the lowest monthly concentrations of nss-K^+ ($1.05 \pm 0.47 \text{ nmol m}^{-3}$) and nss-Ca^{2+} ($2.70 \pm 0.75 \text{ nmol m}^{-3}$) appeared in June 2007 (summer), and the lowest monthly average concentration of nss-SO_4^{2-} ($17.3 \pm 8.15 \text{ nmol m}^{-3}$) was in July 2008 (summer). The seasonal variation trends of nss-K^+ and nss-SO_4^{2-} were consistent with the degree of chlorine depletion, indicating that the chlorine depletion of atmospheric aerosols on Dongsha Island was related to aerosols generated from biomass and fossil fuel combustion.

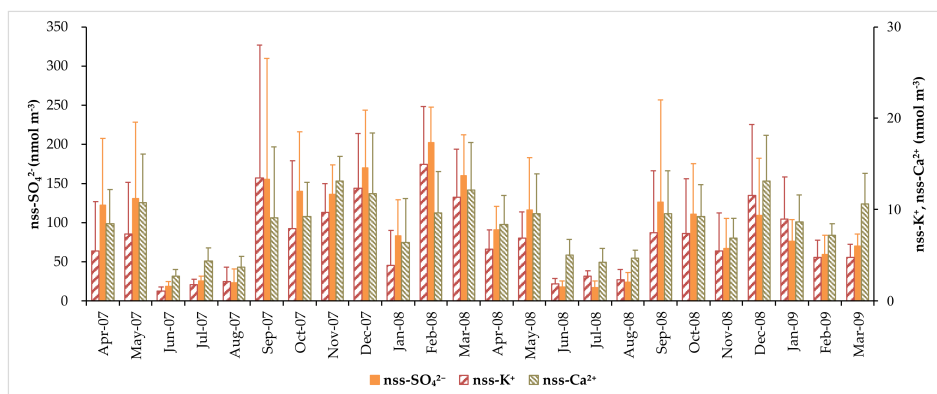


Figure 4. Variations in the monthly average concentrations of non-sea-salt ions.

3.3. Concentrations of Water-Soluble Total Nitrogen (WSTN), Water-Soluble Inorganic Nitrogen (WSIN), and Water-Soluble Organic Nitrogen (WSON) Species

Table 5 indicates that the average concentration of NH_4^+ was $78.4 \pm 67.2 \text{ nmol m}^{-3}$, with the highest monthly average value occurring in September 2007 ($155 \pm 145 \text{ nmol m}^{-3}$) and the lowest in July 2008 ($16.0 \pm 3.37 \text{ nmol m}^{-3}$). The highest and lowest monthly concentrations were accompanied by the relatively high and low concentrations of nss-SO_4^{2-} and nss-K^+ , respectively, indicating the strength of anthropogenic activities. Mainly used in agricultural activities such as animal husbandry and synthetic fertilizers, NH_4^+ can easily form secondary aerosols with sulfates and nitrates [40–42]. In this study, the molar ratio $\text{NH}_4^+/\text{nss-SO}_4^{2-}$ in the atmosphere of the research area was 0.80 (Figure 5), indicating that NH_4^+ on Dongsha Island was chiefly in the form NH_4HSO_4 . Similarly, the molar ratio obtained by [7] in the SCS (1.44) was <2 , indicating that the anthropogenically derived NH_4^+ was insufficient for an NSS sulfate reaction. However, the aforementioned results contradict research conducted by [43] in Beijing and [15] on Huaniao Island, locations that have been heavily influenced by anthropogenic activities. The molar ratios $\text{NH}_4^+/\text{nss-SO}_4^{2-}$ in their studies were 2.50–3.54 (Beijing) and 2.3 (Huaniao Island); these areas are dominated by $(\text{NH}_4)_2\text{SO}_4$ because the anthropogenically derived NH_4^+ in these locations is sufficient for the NSS sulfate reaction.

Table 5. Monthly average concentrations (nmol m^{-3}) of the nitrogen species in TSP samples *.

	NH_4^+	NO_3^-	WSIN #	WSON #	WSTN #
April 2007	66.1 ± 45.3	41.4 ± 12.2	104 ± 54.2	137 ± 32.6	240 ± 80.7
May 2007	115 ± 95.0	48.0 ± 32.0	156 ± 116	115 ± 86.5	271 ± 197
June 2007	19.1 ± 9.32	18.5 ± 7.26	38.2 ± 15.2	40.7 ± 15.2	78.9 ± 25.6
July 2007	21.4 ± 5.86	27.6 ± 7.18	49.4 ± 9.32	40.7 ± 22.0	90.1 ± 20.0
August 2007	27.6 ± 33.9	18.1 ± 8.30	46.0 ± 40.5	50.4 ± 28.1	96.4 ± 68.2
September 2007	155 ± 145	77.7 ± 37.6	201 ± 155	63.8 ± 18.9	265 ± 170
October 2007	118 ± 61.5	81.6 ± 13.6	201 ± 66.7	42.1 ± 24.6	243 ± 69.0
November 2007	107 ± 26.9	70.5 ± 13.8	178 ± 37.5	54.2 ± 22.5	232 ± 46.7
December 2007	130 ± 55.3	74.1 ± 18.8	205 ± 69.0	57.5 ± 14.4	263 ± 78.4
January 2008	77.1 ± 29.1	65.8 ± 20.3	144 ± 43.6	65.4 ± 16.4	209 ± 50.6
February 2008	127 ± 47.7	70.9 ± 26.3	202 ± 75.6	101 ± 32.7	303 ± 101
March 2008	110 ± 48.9	81.4 ± 20.7	205 ± 82.2	159 ± 34.9	363 ± 110
April 2008	52.0 ± 31.6	62.8 ± 21.2	121 ± 46.0	126 ± 23.1	247 ± 59.3
May 2008	110 ± 51.8	52.2 ± 22.6	162 ± 72.8	127 ± 52.3	290 ± 109
June 2008	20.6 ± 11.4	24.6 ± 8.49	45.5 ± 17.6	63.8 ± 24.8	109 ± 36.5
July 2008	16.0 ± 3.37	22.3 ± 6.44	39.0 ± 7.07	61.6 ± 23.0	101 ± 27.8
August 2008	22.8 ± 19.5	22.2 ± 8.60	45.5 ± 25.0	54.7 ± 19.9	100 ± 43.2
September 2008	117 ± 107	56.6 ± 30.1	170 ± 117	83.2 ± 36.0	254 ± 129
October 2008	101 ± 64.6	59.8 ± 26.6	161 ± 89.4	104 ± 31.4	266 ± 113
November 2008	64.8 ± 47.5	62.5 ± 19.2	133 ± 61.8	112 ± 40.0	246 ± 91.2
December 2008	98.9 ± 63.6	79.6 ± 25.4	179 ± 84.3	77.4 ± 27.4	256 ± 101
January 2009	62.9 ± 34.2	76.8 ± 11.9	143 ± 51.7	77.4 ± 27.0	220 ± 42.7
February 2009	73.2 ± 28.3	49.5 ± 21.1	123 ± 46.2	100 ± 28.6	224 ± 73.8
March 2009	68.6 ± 29.7	57.8 ± 18.2	127 ± 42.8	126 ± 29.7	253 ± 50.2
Average	78.4 ± 67.2	54.3 ± 28.7	132 ± 87.9	85.0 ± 46.1	217 ± 115

WSIN, WSON and WSTN represent water-soluble inorganic nitrogen, organic nitrogen (WSON) and total nitrogen (WSTN), respectively. * The daily concentrations of the nitrogen species can be found in Supplementary 2.

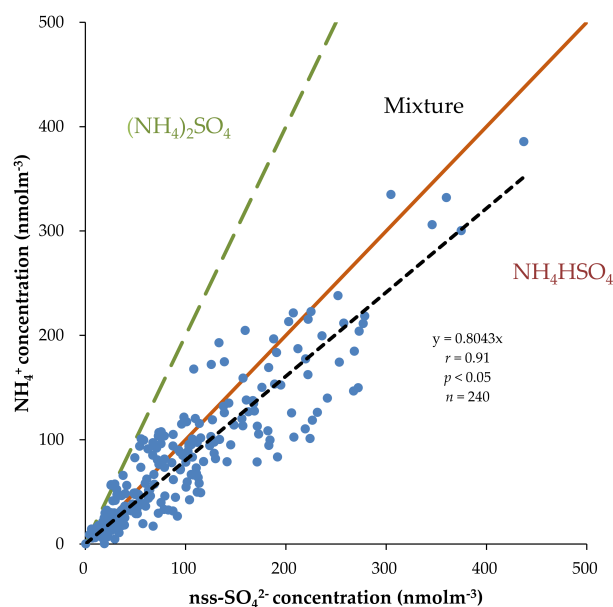


Figure 5. Concentrations of NH_4^+ versus nss-SO_4^{2-} in aerosols; the solid line represents equi-concentration line for NH_4^+ and nss-SO_4^{2-} .

Figure 6 shows that the temporal variation of NO_3^- concentration (average $53.4 \pm 28.7 \text{ nmol m}^{-3}$) in the present study was consistent with that of NH_4^+ , with the highest monthly average value in October 2007 ($81.6 \pm 13.6 \text{ nmol m}^{-3}$) and lowest in August 2007 ($18.1 \pm 8.30 \text{ nmol m}^{-3}$). As a nitrogen oxide (NO_x) generated from fossil fuel combustion, NO_3^- can rapidly form through nitric acid reaction in aerosol and become the main source of atmospheric nitrate [44]. Pryor and Sørensen stated that nitric acid significantly contributes to the deposition of total nitrogen because of its high solubility [45]; specifically, the nitrate in marine environments combines with sea salt particles through atmospheric transmission.

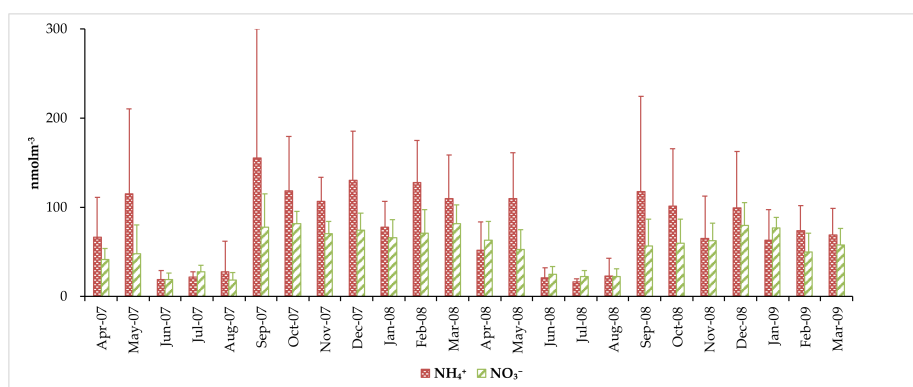


Figure 6. Variations in the monthly average concentrations of NH_4^+ and NO_3^- .

Figure 7 reveals that the seasonal variations of WSIN, WSON, and WSTN exhibited similar trends. The average concentrations of WSIN, WSON, and WSTN were 132 ± 87.9 , 85 ± 46 , and $217 \pm 115 \text{ nmol m}^{-3}$, respectively. The WSIN, WSON, and WSTN mostly originated from northern sources, and the highest monthly average concentration usually occurred in spring or winter. By contrast, the lowest monthly average concentration usually occurred in summer, at which point the WSIN, WSON, and WSTN had southern sources. Recorded concentrations of WSTN collected in the Asian marginal sea area (Table 6; Figure 8) range from approximately 50 to 350 nmol m^{-3} , with the highest value of 321 nmol m^{-3} [46] collected in the East China Sea, which was mainly affected by the emission of anthropogenically derived Nr species in China. The remaining concentrations are as follows, presented in descending order: 196 nmol m^{-3} in the SCS [20]; 91 nmol m^{-3} in the north-west Pacific Ocean [47]; and 58 nmol m^{-3} in the Bay of Bengal [48].

Table 6. Nitrogen species concentration in atmospheric suspended particle from different sites around the world.

Sampling Periods	Location	Station Type	WSIN		WSON		WSTN	Reference
			nmol m ⁻³	%	nmol m ⁻³	%	nmol m ⁻³	
May 2007–July 2009	Miami, USA	Coastal city	51 ± 26	96 ± 69	2.4 ± 3.1	4 ± 6	53 ± 26	[49]
August–September 2007 & 2008	Barbados, Atlantic Ocean	Island	20 ± 8.8	94 ± 57	1.3 ± 1.5	6 ± 7	21 ± 8.9	[49]
March 2014–April 2015	Erdemli, Turkey	Coastal city	40 ± 28	63 ± 54	24 ± 16	37 ± 32	64 ± 33	[50]
August 2003–September 2005	Eilat, Israel	Coastal city	65 ± 24	89 ± 47	8 ± 5	11 ± 8	73 ± 28	[51]
March–April 2006	northern Indian Ocean	Marginal sea	47	81	11	19	58	[48]
May 2007–Oct 2009	western Pacific Ocean	Open ocean	11 ± 4.8	72 ± 39	4.3 ± 1.7	28 ± 15	15 ± 5.1	[52]
March–April 2014	northwestern Pacific Ocean	Open ocean	80 ± 55	88 ± 80	11 ± 7	12 ± 11	91 ± 55	[47]
April 2010–November 2012	Rishiri Island, Japan	Island	35 ± 11	86 ± 37	5.5 ± 4.1	14 ± 11	41 ± 12	[53]
March–April 2006	Qindao, China	Coastal city	783	81	180	19	963	[20]
January–July 2013	Beijing, China	Inland city	758	79	204	21	962	[54]
July 2008–August 2009	Xian, China	Inland city	377 ± 349	56 ± 71	300 ± 263	44 ± 55	677 ± 594	[55]
March–May 2015	East China Sea	Marginal sea	219	68	102	32	321	[46]
January–December 2006	Keelung, Taiwan	Coastal city	213 ± 81	74 ± 38	76 ± 28	26 ± 13	289 ± 102	[17]
September 2015–March 2017	Daya Bay, China	Coastal city	19 ± 18	36 ± 40	33 ± 22	63 ± 56	52 ± 29	[56]
August 2013–May 2014	Guangzhou, China	Coastal city	260 ± 180	86 ± 81	43 ± 32	14 ± 11	303 ± 196	[57]
April–May 2005	South China Sea	Marginal sea	131	67	65	33	196	[20]
March–April 2007	Singapore	Coastal city	98 ± 35	70 ± 35	43 ± 27	30 ± 22	141 ± 50	[58]
April 2007–March 2009	Dongsha, Taiwan	Island	132 ± 88	63 ± 53	79 ± 42	37 ± 27	211 ± 112	This study

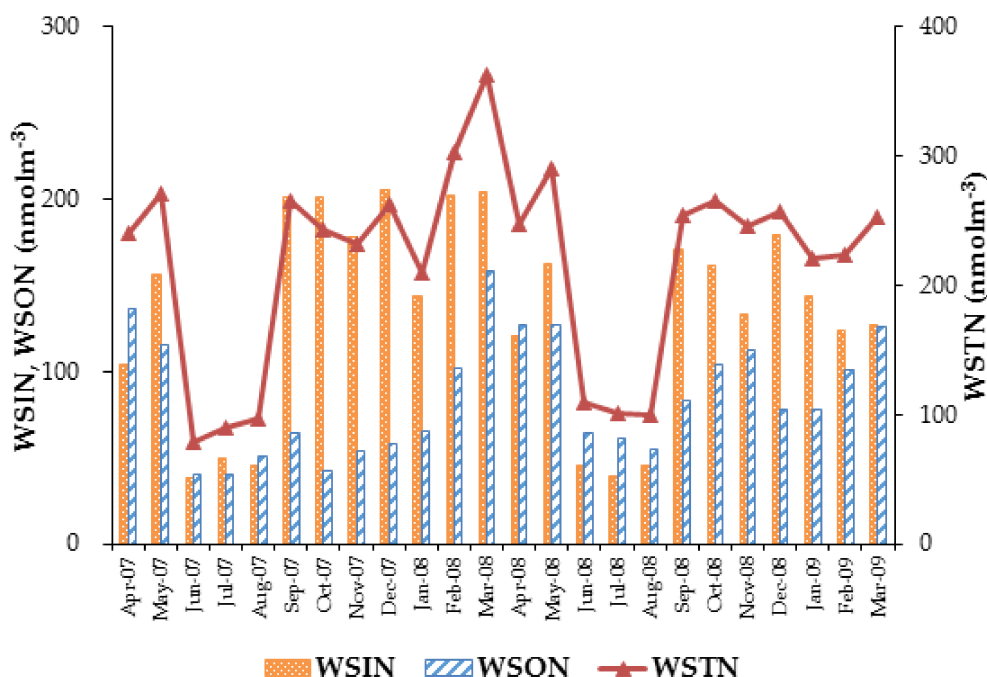


Figure 7. Variations in the monthly average concentrations of WSIN, WSON and WSTN.

For locations north of 30° N in Asia, particularly in China, the recorded average WSTN concentrations range from approximately 300 to 1000 nmol m⁻³: 962 nmol m⁻³ in Beijing [54], 963 nmol m⁻³ in Qingdao [20], and 677 ± 594 nmol m⁻³ in Xi'an [55]. These results indicate that China emits large amounts of Nr from industrial activities. Compared with China, Jeju Island in Korea [59] and Rishiri Island in Japan [53] have relatively low concentrations of WSTN. For locations south of 30° N in Asia, the WSTN concentration ranges from approximately 50 to 300 nmol m⁻³: 303 ± 196 nmol m⁻³ in Guangzhou [57]; 289 ± 102 nmol m⁻³ in Keelung [17]; 211 ± 112 nmol m⁻³ on Dongsha Island; 141 ± 50 nmol m⁻³ in Singapore [58]; and 52 ± 29 nmol m⁻³ in Daya Bay [56].

From the aforementioned results, WSTN concentrations in Asia gradually diminish from north to south, with China exhibiting the highest concentrations, mainly induced by direct or indirect emissions from anthropogenic activities. The majority of locations north of 30° N exhibited an organic nitrogen ratio of <20% (10–20%), except for the East China Sea (32%) [46]. Locations south of 30° N exhibited an organic nitrogen ratio of 14–39%, with the majority of locations having a ratio >30%, except for Guangzhou (14%) [57]. Notably, the worldwide organic to total nitrogen ratio is approximately 26–30% [60,61], which is higher than that in locations north of 30° N. A possible explanation is excessive concentrations of inorganic nitrogen, which caused the ratio of organic nitrogen to decrease; this shows that anthropogenic activities in China contribute considerably to nitrogen deposition in the surrounding marine ecosystem.

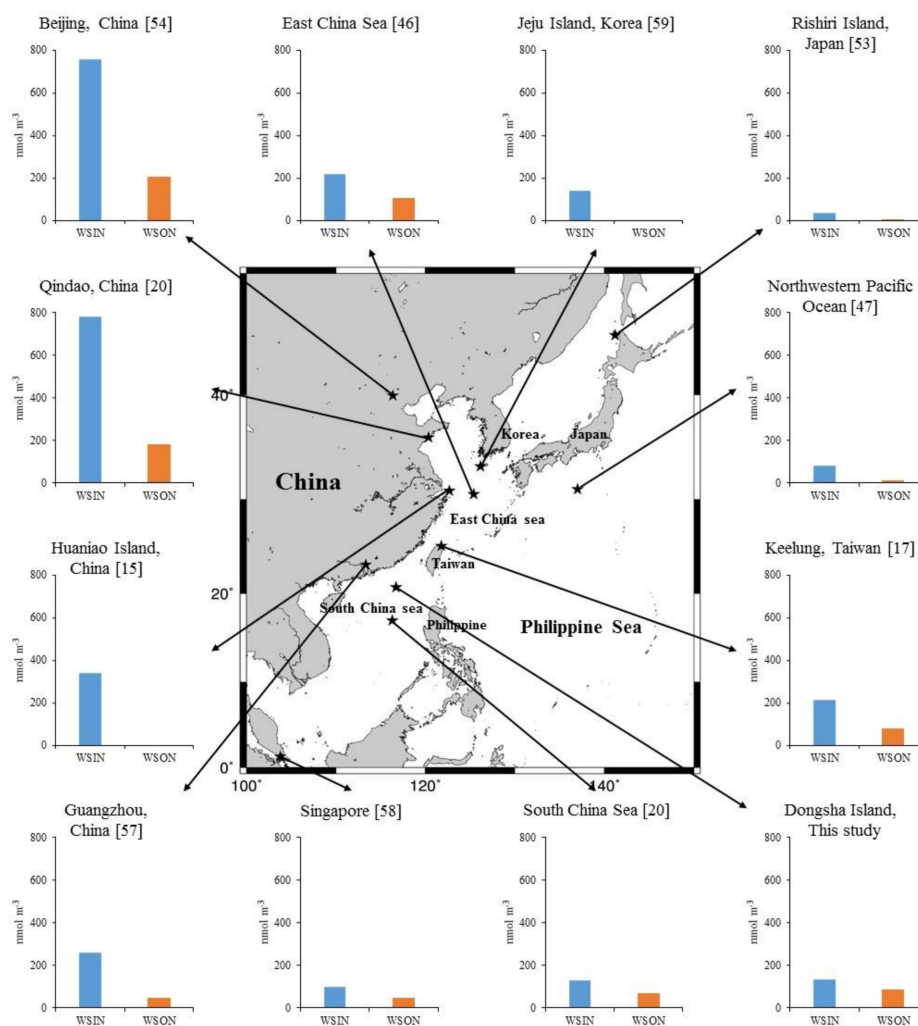


Figure 8. Comparison of WSIN and WSON in aerosols between Dongsha Island and around East Asia.

3.4. Correlation Analysis and Principal Component Analysis (PCA)

To determine the correlations among species, IBM SPSS Statistics 22 was employed for correlation analysis. Table 7 shows that there was strong correlation among sea salt ions (Na^+ , Mg^{2+} , and Cl^- ; $r = 0.92\text{--}0.99$), and sea salt ions were also significantly correlated with wind speed ($r = 0.72\text{--}0.82$). Thus, seawater was the main source of sea salt ions. High wind speed causes seawater to form sea salt particles, which further affects the concentration of sea salt ions. The correlation between Ca^{2+} and sea salt ions was relatively strong ($r = 0.65\text{--}0.77$), and Ca^{2+} was highly correlated with nss-Ca^{2+} ($r = 0.87$) and wind speed ($r = 0.71$); nss-Ca^{2+} originates from crustal sources and is especially susceptible to influence by Asian dust in the spring [7]. This result is consistent with that obtained in a study by [31] on aerosols in the southern East China Sea, indicating that terrestrial substances from continental Asia can reach the SCS. K^+ was moderately correlated with sea salt ions ($r = 0.41\text{--}0.64$), highly correlated with nss-K^+ ($r = 0.89$), and moderately correlated with wind speed ($r = 0.62$), which indicates that aerosols within this region are also affected by biomass combustion [38]. SO_4^{2-} was strongly correlated with nss-SO_4^{2-} ($r = 0.99$) and moderately correlated with wind speed ($r = 0.41$), suggesting that aerosols within this region are affected by fossil fuel combustion. Chlorine depletion was highly correlated with nss-K^+ ($r = 0.62$) and nss-SO_4^{2-} ($r = 0.73$), indicating that aerosols within this area are still affected by anthropogenic activities despite the >100 km distance from continental Asia.

WSTN was highly correlated with nitrogen species ($r = 0.72\text{--}0.93$), with $r = 0.72$ for WSTN and WSON and $r = 0.93$ for WSTN and WSIN. By contrast, WSON and WSIN were moderately correlated

($r = 0.41$). WSIN was highly correlated with NO_3^- ($r = 0.88$) and NH_4^+ ($r = 0.96$). Except for WSON ($r = 0.39$), chlorine depletion was well correlated with other nitrogen species ($r = 0.57$ – 0.66); this disparity may be a result of the complex sources of WSON. In addition, nss-SO_4^{2-} was positively correlated with nitrogen species ($r = 0.40$ – 0.91), exhibiting a moderate correlation with WSON ($r = 0.40$) and strong correlation with NH_4^+ ($r = 0.91$). Because nss-SO_4^{2-} is an indicator of fossil fuel combustion, this result was presumably affected by the products of anthropogenic activities, which were transported by the north-east monsoon. The correlation coefficient between nss-Ca^{2+} and nitrogen species ranged from 0.39 to 0.78, with the highest correlation being between nss-Ca^{2+} and WSIN ($r = 0.78$); this indicates that WSIN is related to continental substances. The correlations between nss-K^+ and nitrogen species were 0.29–0.84, with the highest correlation being between nss-K^+ and NH_4^+ ($r = 0.84$), suggesting that biomass combustion was a primary source. According to the correlation analysis of nitrogen species and major ions, the sources of WSON might be more complicated than and differ from those of other nitrogen species.

To further understand the source of nitrogen species in aerosols of the region, Statistica version 12 was used to conduct principal component analysis (PCA), the results of which are presented in Table 8. The objective was to distinguish possible sources of TSPs in the northern SCS. Three factors were extracted, and variables with a factor loading >0.8 were considered sufficient to explain the significance of the principal components in this study. The variables in factor 1 consisted of NH_4^+ , NO_3^- , WSIN, SO_4^{2-} , K^+ , Ca^{2+} , nss-SO_4^{2-} , nss-K^+ , and nss-Ca^{2+} , and the total variance explained was 62.2%. NO_3^- (-0.87) and nss-SO_4^{2-} (-0.91) are generally considered products of fossil fuel combustion; nss-K^+ (-0.86) is an indicator of biomass combustion; NH_4^+ (-0.88) originates from fertilizer use and livestock waste [20]; and nss-Ca^{2+} (-0.87) has crustal sources. Therefore, factor 1 was classified as components of fossil fuel and biomass combustion and crustal sources. The explained variance for factor 2 was 20.5%; the variables contained marine source indicators including the ions Na^+ (0.86), Cl^- (0.94), and Mg^{2+} (0.82); therefore, factor 2 was classified as marine sources [31]. The partial explained variance for factor 3 was 6.4%, and the only variable was WSON (0.84). The factor loadings for WSON in factors 1 and 2 were -0.46 and -0.22 , respectively, indicating that the air mass sources of WSON in aerosols of the SCS were relatively complex [32] and rarely affected by marine or crustal sources. The total explained variance, which was 89.1% (Figure 9), contained factors 1 (continental sources), 2 (marine sources), and 3 (general sources), indicating the complexity of aerosol sources in the SCS. In summary, the results of PCA revealed that continental and anthropogenic aerosols have a considerable effect on the SCS. Understanding the mechanism of WSON formation provides a more comprehensive explanation of the sources and compositions of aerosols.

Table 7. Correlation matrix of the species in TSP samples.

	NO ₃ ⁻	NH ₄ ⁺	WSIN	WSON	WSTN	Na ⁺	Mg ²⁺	Cl ⁻	K ⁺	Ca ²⁺	SO ₄ ²⁻	nss-K ⁺	nss-Ca ²⁺	nss-SO ₄ ²⁻	Cl ⁻ Depletion	Wind Speed
NO ₃ ⁻	1															
NH ₄ ⁺	0.77 **	1														
WSIN	0.88 **	0.96 **	1													
WSON	0.39 **	0.35 **	0.41 **	1												
WSTN	0.83 **	0.88 **	0.93 **	0.72 **	1											
Na ⁺	0.42 **	0.14 **	0.26 **	0.07	0.23 **	1										
Mg ²⁺	0.47 **	0.21 **	0.33 **	0.11	0.30 **	0.99 **	1									
Cl ⁻	0.25 **	-0.05	0.06	-0.03	0.04	0.94 **	0.92 **	1								
K ⁺	0.76 **	0.76 **	0.81 **	0.27 **	0.73 **	0.59 **	0.64 **	0.41 **	1							
Ca ²⁺	0.70 **	0.58 **	0.67 **	0.30 **	0.63 **	0.77 **	0.82 **	0.65 **	0.85 **	1						
SO ₄ ²⁻	0.76 **	0.90 **	0.90 **	0.40 **	0.84 **	0.34 **	0.40 **	0.12	0.86 **	0.70 **	1					
nss-K ⁺	0.69 **	0.84 **	0.84 **	0.29 **	0.76 **	0.14 **	0.21 **	-0.04	0.89 **	0.59 **	0.85 **	1				
nss-Ca ²⁺	0.71 **	0.74 **	0.78 **	0.39 **	0.75 **	0.37 **	0.44 **	0.22 **	0.79 **	0.87 **	0.76 **	0.76 **	1			
nss-SO ₄ ²⁻	0.73 **	0.91 **	0.90 **	0.40 **	0.85 **	0.23 **	0.29 **	0.01	0.81 **	0.63 **	0.99 **	0.86 **	0.75 **	1		
Cl ⁻ depletion	0.57 **	0.64 **	0.66 **	0.39 **	0.66 **	0.17 **	0.20 **	-0.12	0.59 **	0.42 **	0.72 **	0.62 **	0.49 **	0.73 **	1	
Wind speed	0.53 **	0.25 **	0.39 **	0.11	0.34 **	0.82 **	0.82 **	0.72 **	0.62 **	0.71 **	0.41 **	0.29 **	0.41 **	0.33 **	0.24 **	1

** Correlation is significant at the 0.01 level (2-tailed); * Correlation is significant at the 0.05 level (2-tailed).

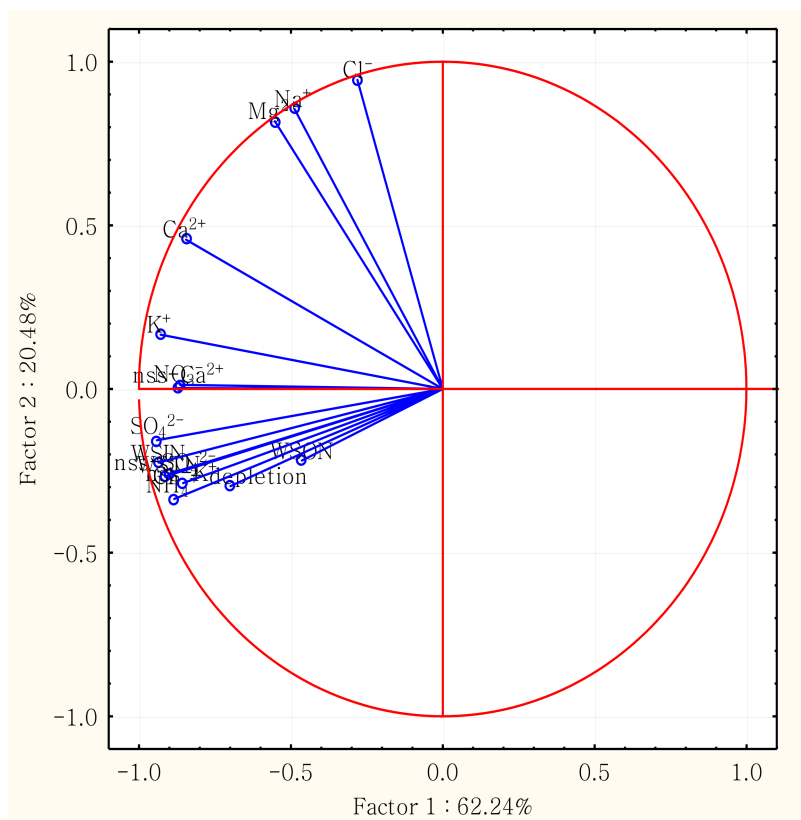


Figure 9. Projection of the variables on the factor plane 1 × 2 of the principal component analysis (PCA).

Table 8. Varimax-rotated factor matrix and corresponding probable sources of the northern South China Sea aerosols.

	Factor 1	Factor 2	Factor 3
NH ₄ ⁺	−0.884	−0.336	0.139
NO ₃ [−]	−0.871	0.003	0.048
WSIN	−0.936	−0.224	−0.047
WSON	−0.464	−0.218	0.840
WSTN	−0.903	−0.260	0.301
Cl [−]	−0.281	0.944	0.050
Na ⁺	−0.488	0.855	0.044
Mg ²⁺	−0.553	0.818	0.049
SO ₄ ^{2−}	−0.941	−0.157	−0.102
K ⁺	−0.929	0.166	0.193
Ca ²⁺	−0.845	0.456	0.003
nss-SO ₄ ^{2−}	−0.915	−0.267	−0.111
nss-K ⁺	−0.855	−0.287	0.261
nss-Ca ²⁺	−0.865	0.013	−0.030
Cl [−] depletion %	−0.699	−0.297	0.037
Eigenvalue	9.336	3.072	0.957
% Total variance	62.24	20.48	6.38
Cumulative %	62.24	82.72	89.10
Probable source	Combustion, Biomass burning and crustal sources	Marine source	Combined sources

3.5. Fluxes of Nitrogen Species

To determine the effects of the atmospheric transmission of nitrogen species on the biogeochemistry of the SCS, this study quantified the input of nitrogen species by calculating the dry deposition flux. The formula for flux (F in unit of $\mu\text{mol m}^{-2} \text{d}^{-1}$) estimation is as follows [47]:

$$F = C_d \times V_d \tag{9}$$

where C_d denotes the concentration of the water-soluble nitrogen species (mmol m^{-3}) and V_d represents the deposition rate of aerosols (cm s^{-1}).

Hoppel et al. indicated that particle size ranges from 0.1 to 100 μm , and the rate of dry deposition can vary by three orders of magnitude [62]. In general, NH_4^+ concentrates on particles of size 0.1–1 μm , whereas the majority of NO_3^- is coarse particles of 1–10 μm [62]. However, any compound or element calculated using a fixed deposition rate may cause underestimation or overestimation of the flux [40]. The samples collected in this study were total suspended particle (TSP), the particle size of which is indistinguishable according to models and experiments with aerosol deposition on ocean surfaces and the size distribution of NO_3^- and NH_4^+ in particles [31,62–64]. In the present study, the deposition rates of NO_3^- and NH_4^+ were taken as 1.2 and 0.1 cm s^{-1} , respectively [65,66]. The flux of WSIN was defined as the sum of the NO_3^- and NH_4^+ fluxes.

Lesworth et al. and Srinivas et al. revealed that the particle size distribution of WSON is wide-ranging [67,68]. This is because 1 cm s^{-1} is similar to the deposition rate of the top layer of the atmospheric boundary layer; thus, obtained WSON flux can represent the top layer of the atmospheric boundary layer [47]. In addition, Chen et al. noted that the ratio of coarse to fine particles (C/F ratio) for WSON is 0.88. The deposition rates of coarse and fine particles (i.e., 2 and 0.1 cm s^{-1}) can be employed to derive the deposition rate ($\sim 1 \text{ cm s}^{-1}$) of WSON in TSPs, indicating that this deposition rate is optimal for estimating the dry deposition flux of WSON [32].

During the study period, the average daily flux of WSTN on Dongsha Island (Table 9) was $137 \pm 62.1 \mu\text{mol m}^{-2} \text{ d}^{-1}$, of WSIN was $63.0 \pm 34.4 \mu\text{mol m}^{-2} \text{ d}^{-1}$, and of WSON was $73.5 \pm 39.9 \mu\text{mol m}^{-2} \text{ d}^{-1}$, yielding a ratio of 46:54 as the flux of WSIN to WSON. If the flux was estimated based on its air mass source, WSTN with northern sources reached $167 \pm 50.4 \mu\text{mol m}^{-2} \text{ d}^{-1}$, southern sources reached $79.0 \pm 35.5 \mu\text{mol m}^{-2} \text{ d}^{-1}$, and marine sources reached $73.3 \pm 19.1 \mu\text{mol m}^{-2} \text{ d}^{-1}$. The WSTN flux of the northern air masses was more than two times those of the southern and marine air masses, indicating that the atmospheric WSTN on Dongsha Island originated from terrigenous materials or anthropogenic activities from northern sources, and the flux ratio of northern, southern, and marine sources was approximately 80:18:2.

Table 9. Daily average fluxes ($\mu\text{mol m}^{-2} \text{ day}^{-1}$) of the nitrogen species in TSP samples.

	WSTN	WSON	WSIN
April 2007	167 ± 36.9	118 ± 28.2	48.7 ± 16.1
May 2007	159 ± 110	99.4 ± 74.8	59.7 ± 40.4
June 2007	56.0 ± 18.3	35.2 ± 13.1	20.9 ± 8.10
July 2007	65.6 ± 14.5	35.2 ± 19.0	30.4 ± 7.46
August 2007	64.7 ± 34.9	43.5 ± 24.3	21.2 ± 11.0
September 2007	149 ± 63.2	55.2 ± 16.4	94.0 ± 50.4
October 2007	131 ± 24.2	36.3 ± 21.3	94.8 ± 16.5
November 2007	129 ± 29.2	46.8 ± 19.4	82.3 ± 15.9
December 2007	138 ± 31.8	49.7 ± 12.5	88.1 ± 22.8
January 2008	131 ± 28.0	56.5 ± 14.2	74.9 ± 22.5
February 2008	172 ± 52.0	87.6 ± 28.2	84.5 ± 30.8
March 2008	231 ± 48.7	137 ± 30.2	93.9 ± 25.2
April 2008	179 ± 36.9	109 ± 20.0	69.6 ± 24.1
May 2008	174 ± 65.3	110 ± 45.2	63.6 ± 27.6
June 2008	82.5 ± 28.7	55.1 ± 21.4	27.3 ± 9.40
July 2008	77.8 ± 24.2	53.2 ± 19.9	24.5 ± 6.66
August 2008	72.2 ± 26.1	47.2 ± 17.2	25.0 ± 9.80
September 2008	141 ± 58.2	71.9 ± 31.1	68.8 ± 39.1
October 2008	161 ± 56.0	90.1 ± 27.1	70.8 ± 32.7
November 2008	168 ± 54.1	97.2 ± 34.6	70.4 ± 23.6
December 2008	158 ± 49.1	66.8 ± 23.7	91.0 ± 30.7
January 2009	152 ± 20.8	66.8 ± 23.3	85.0 ± 14.7
February 2009	144 ± 47.8	86.8 ± 24.7	57.6 ± 23.7
March 2009	174 ± 37.3	109 ± 25.7	65.9 ± 20.4
Average	137 ± 62.1	73.5 ± 39.9	63.0 ± 34.4

According to nitrogen flux data obtained globally, the WSIN flux in the pelagic zone is relatively low at $2.6 \text{ mmol m}^{-2} \text{ y}^{-1}$ [40] in the Atlantic Ocean; $1.1 \text{ mmol m}^{-2} \text{ y}^{-1}$ [69] in the central Pacific Ocean; and $0.8 \text{ mmol m}^{-2} \text{ y}^{-1}$ [69] in the southern Pacific Ocean. By contrast, the WSTN flux in marginal areas of the north-western Pacific Ocean can reach up to $21 \text{ mmol m}^{-2} \text{ y}^{-1}$ [47]. The fluxes of these oceans were all lower than that of the SCS ($50 \pm 23 \text{ mmol m}^{-2} \text{ y}^{-1}$), which may be because of the effect of the monsoon patterns, which bring large amounts of terrigenous and anthropogenic materials to the SCS.

The WSTN flux in East Asia (Table 10) is relatively high in the Pearl River Delta regions of southern China, such as Dinghu Mountain ($104 \text{ mmol m}^{-2} \text{ y}^{-1}$) and the Hengmen area ($96 \text{ mmol m}^{-2} \text{ y}^{-1}$) [70]. Because these locations are inland north of the SCS, they are most directly affected by anthropogenic activities. The WSTN flux in the southern East China Sea was measured at $61 \text{ mmol m}^{-2} \text{ y}^{-1}$ [17], whereas that in Singapore, located at the southern end of the SCS, was $54 \pm 19 \text{ mmol m}^{-2} \text{ y}^{-1}$ [58]. Because these two locations both belong to densely populated areas, they exhibit a higher flux than that recorded in the northern SCS in this study ($50 \pm 23 \text{ mmol m}^{-2} \text{ y}^{-1}$). The decreasing distribution of nitrogen flux in the offshore area in Asia indicates that atmospheric N_r is mainly affected by terrigenous materials and anthropogenic activities.

Table 10. Nitrogen species fluxes ($\text{mmol m}^{-2} \text{ yr}^{-1}$) in dry deposition from different site around the East Asia.

Sampling Periods	Location	Station Type	NO ₃ ⁻	NH ₄ ⁺	WSIN	WSO _N	WSTN	Reference
March–April 2014	North-western Pacific Ocean	Open ocean	16 ± 20	1.7 ± 1.4	18 ± 20	2.8 ± 2.4	21 ± 22	[47]
March–May 2015	North-western Pacific Ocean	Open ocean	8.0	0.5	8.5	4.0	12.5	[46]
April 2010–March 2011	Huaniao, China	Island	37	4.35	41.35			[15]
January–December 2007	Dinghushan, China	Coastal city	26	52	78	26	104	[70]
November 2006–October 2007	Hengmen, China	Coastal city	27	39	66	30	96	[70]
September 2015–March 2017	Daya Bay, China	Coastal city	8.46	0.93	9.44	16.33	25.77	[56]
January–December 2006	Keelung, Taiwan	Coastal city	5.6 ± 1.4	34 ± 15	39 ± 17	22 ± 9	61 ± 19	[17]
July 2010–March 2011	Dongsha, Taiwan	Island	16 ± 14	7 ± 5	23 ± 15			[21]
April 2007–March 2009	Dongsha, Taiwan	Island	21 ± 11	2.5 ± 2.1	23 ± 13	27 ± 15	50 ± 23	This study
March–April 2007	Singapore	Coastal city	18 ± 5.7	10 ± 6.4	28 ± 8.6	16 ± 10	54 ± 19	[58]

3.6. Contribution of Atmospheric N Deposition to New Production in the South China Sea (SCS)

Oligotrophic open sea areas constitute the majority of global surface seawater (~75%), accounting for more than 30% of global carbon fixation. These oligotrophic water bodies contribute substantially to the global carbon cycle [71]. The transmission flux of particulate organic carbon acts as a physical and biological pump for carbon dioxide by storing it deep in the ocean; thus, such flux plays a vital role in the transmission of carbon dioxide from the atmosphere to the oceans [72]. The deposition of atmospheric N_r species forms the external nitrogen supply of the SCS. Specifically, the effects of the prevailing north-east monsoon and anthropogenic activities enable atmospheric nitrogen deposition to bring new external production to the marine ecosystem of the SCS.

Yan and Kim used the bioavailability of nitrogen species to estimate the flux of new marine production induced by atmospheric deposition [73], with organic nitrogen accounting for 20%–80% and inorganic nitrogen for 100%. The present study calculated that the N_r species in atmospheric dry deposition can provide seawater with $28.4\text{--}44.5 \text{ mmol N m}^{-2} \text{ y}^{-1}$ of primary production. A C/N ratio of 6.625 in the Redfield ratio was used for conversion of the new production of the ocean's external nitrogen supply, which was approximately $0.52\text{--}0.81 \text{ mmol C m}^{-2} \text{ d}^{-1}$. Li et al. collected deposition particles in sea areas near Dongsha Island using a drifting sediment trap and analyzed the concentration of particulate organic carbon; they calculated the flux to be $9.24 \pm 0.89 \text{ mmol C m}^{-2} \text{ d}^{-1}$ [74]. Based on this figure, the input of the ocean's external nitrogen supply contributes 5.6–8.7% of new production to the ocean in the northern SCS. According to examination of the primary air mass source of atmospheric input for the ocean's external nitrogen supply, new production when air masses were from northern sources was $36.1\text{--}54.8 \text{ mmol N m}^{-2} \text{ y}^{-1}$ ($0.65\text{--}0.99 \text{ mmol C m}^{-2} \text{ d}^{-1}$), with a contribution of 7.1–10.8%. The new production for southern sources was $13.9\text{--}25.1 \text{ mmol N m}^{-2} \text{ y}^{-1}$ ($0.25\text{--}0.46 \text{ mmol C m}^{-2} \text{ d}^{-1}$), with a contribution of 2.7–4.9%, and that for marine sources was $12.9\text{--}23.3 \text{ mmol N m}^{-2} \text{ y}^{-1}$ ($0.23\text{--}0.42 \text{ mmol C m}^{-2} \text{ d}^{-1}$), with a contribution of 2.5–4.6%. The results show that the contribution of

northern sources was greater than that of southern and marine sources, with a maximum contribution of approximately 10%. Research in other parts of the world has found that the new production contribution caused by the nitrogen species of atmospheric dry deposition can reach 28% in the north-west Mediterranean [75], 25% in the Bay of Bengal [48], and approximately 8.2% in the southern East China Sea [17].

4. Conclusions

This study estimated the sources of atmospheric nitrogen species and their effects on the nitrogen cycle in the northern SCS. The results indicated that the chemical composition of atmospheric particles in this region is significantly affected by the output from northern continental Asia (mainly in spring and winter). In addition, comparisons between the results of this study and those in the literature indicated that the concentration of water-soluble nitrogen species in East Asia diminishes from north to south, with the highest concentration in northern China. The north and south also exhibited a gap in ratio of organic to total nitrogen; the percentage was <20% for locations north of 30° N and >30% for those south of 30° N. This finding shows that the concentration of organic nitrogen increases from north to south because of the relatively high concentration of inorganic nitrogen in the north. Furthermore, this study determined that the molar ratio $\text{NH}_4^+/\text{nss-SO}_4^{2-}$ is 0.80, demonstrating that NH_4^+ on Dongsha Island is mainly in the form of NH_4HSO_4 because anthropogenically derived NH_4^+ on Dongsha Island does not provide a sufficient amount for nss-SO_4^{2-} reactions.

Correlation analysis revealed a significant correlation between sea salt ions (Na^+ , Mg^{2+} , and Cl^-), and between sea salt ions and wind speed ($r = 0.72\text{--}0.99$), indicating that windblown sea spray is the main source of sea salt ions in the northern SCS. However, the correlation between sea salt ions and nitrogen species was weak ($r < 0.50$), indicating that marine sources were not the main origin of nitrogen species. The highest correlation coefficient was that between nss-Ca^{2+} and WSIN ($r = 0.78$), indicating that the source of WSIN was substances in the continental crust. The correlation between nss-K^+ and NH_4^+ ($r = 0.84$) was the strongest, indicating that its source was related to biomass combustion. Moderate correlation was observed between nss-SO_4^{2-} and WSIN ($r = 0.73\text{--}0.91$), implying that its source was fossil fuel combustion. Furthermore, PCA indicated that fossil fuel and biomass combustion and crustal substances were the primary sources of inorganic nitrogen species and NSS ions. In addition, sea salt ions with marine sources accounted for a significant proportion of aerosols in the region. By contrast, the sources of organic nitrogen species were relatively complex.

During the research period, the daily average flux of WSTN in the atmospheric aerosol of the northern SCS was $137 \pm 62.1 \mu\text{mol m}^{-2} \text{d}^{-1}$, and the flux ratio of WSIN to WSON was approximately 46:54. The atmospheric input of the ocean's external nitrogen supply to the waters of the region engendered a new production rate of $0.52\text{--}0.81 \text{ mmol C m}^{-2} \text{d}^{-1}$ and contributed to 5.6–8.7% of new production in the northern SCS. Northern sources contributed up to 7.1–10.8% of new production, whereas southern and marine sources accounted for 2.7–4.9% and 2.5–4.6%, respectively. This result indicates that the ocean's external nitrogen supply, provided by anthropogenic aerosols, is vital for the biogeochemical cycle in Asian marginal seas, particularly the northern SCS.

Supplementary Materials: The following are available online at <http://www.mdpi.com/2073-4433/9/10/386/s1>, Table S1: Daily wind speeds (m/s) and concentrations (nmol m^{-3}) of major ions and non-sea-salt (nss) ions and in TSP samples, and Table S2: Daily concentrations (nmol m^{-3}) of nitrogen species in TSP samples.

Author Contributions: Data curation, S.Z.-H.; Methodology, S.Z.-H.; Writing—original draft, H.-Y.C. and S.Z.-H.; Writing—review and editing, H.-Y.C.

Funding: Ministry of Science and Technology, Taiwan: MOST106-2611-M-019-020

Acknowledgments: The Ministry of Science and Technology of the Republic of China (grant MOST 106-2611-M-019-020) is acknowledged for the financial support. The research was also partly supported by the Center of Excellence for the Oceans, National Taiwan Ocean University. Our special thanks go to Fei-Jan Lin for his help with TSP sampling and to the editor and two anonymous reviewers for their helpful comments and suggestions.

References

1. Boreddy, S.K.R.; Kawamura, K. A 12-year observation of water-soluble ions in TSP aerosols collected at a remote marine location in the western North Pacific: An outflow region of Asian dust. *Atmos. Chem. Phys.* **2015**, *15*, 6437–6453. [[CrossRef](#)]
2. Arakaki, T.; Azechi, S.; Somada, Y.; Ijyu, M.; Nakaema, F.; Hitomi, Y.; Handa, D.; Oshiro, Y.; Miyagi, Y.; Tsuchioka, A.; et al. Spatial and temporal variations of chemicals in the TSP aerosols simultaneously collected at three islands in Okinawa, Japan. *Atmos. Environ.* **2014**, *97*, 479–485. [[CrossRef](#)]
3. Jickells, T. The role of air-sea exchange in the marine nitrogen cycle. *Biogeosciences* **2006**, *3*, 271–280. [[CrossRef](#)]
4. Wang, H.; Wang, X.; Yang, X.; Li, W.; Xue, L.; Wang, T.; Chen, J.; Wang, W. Mixed Chloride Aerosols and their Atmospheric Implications: A Review. *Aerosol Air Qual. Res.* **2017**, *17*, 878–887. [[CrossRef](#)]
5. Kawakami, N.; Osada, K.; Nishita, C.; Yabuki, M.; Kobayashi, H.; Hara, K.; Shiobara, M. Factors controlling sea salt modification and dry deposition of nonsea-salt components to the ocean. *J. Geophys. Res.* [[CrossRef](#)]
6. Yao, X.; Zhang, L. Chemical processes in sea-salt chloride depletion observed at a Canadian rural coastal site. *Atmos. Environ.* **2012**, *46*, 189–194. [[CrossRef](#)]
7. Hsu, S.C.; Liu, S.C.; Kao, S.J.; Jeng, W.L.; Huang, Y.T.; Tseng, C.M.; Tsai, F.; Tu, J.Y.; Yang, Y. Water-soluble species in the marine aerosol from the northern South China Sea: High chloride depletion related to air pollution. *J. Geophys. Res.* **2007**, *112*. [[CrossRef](#)]
8. Yao, X.; Fang, M.; Chan, C.K. The size dependence of chloride depletion in fine and coarse sea-salt particles. *Atmos. Environ.* **2003**, *37*, 743–751. [[CrossRef](#)]
9. Galloway, J.N.; Townsend, A.R.; Erisman, J.W.; Bekunda, M.; Cai, Z.; Freney, J.R.; Martinelli, L.A.; Seitzinger, S.P.; Sutton, M.A. Transformation of the Nitrogen Cycle: Recent Trends, Questions, and Potential Solutions. *Science* **2008**, *320*, 889–892. [[CrossRef](#)] [[PubMed](#)]
10. Fowler, D.; Coyle, M.; Skiba, U.; Sutton, M.A.; Cape, J.N.; Reis, S.; Sheppard, L.J.; Jenkins, A.; Grizzetti, B.; Galloway, J.N.; et al. The global nitrogen cycle in the twenty-first century. *Philos. Trans. R. Soc. Lond. B Biol. Sci.* **2013**, *368*, 20130164. [[CrossRef](#)] [[PubMed](#)]
11. Gu, B.; Ju, X.; Chang, J.; Ge, Y.; Vitousek, P.M. Integrated reactive nitrogen budgets and future trends in China. *Proc. Natl. Acad. Sci. USA* **2015**, *112*, 8792–8797. [[CrossRef](#)] [[PubMed](#)]
12. Liu, X.; Zhang, Y.; Han, W.; Tang, A.; Shen, J.; Cui, Z.; Vitousek, P.; Erisman, J.W.; Goulding, K.; Christie, P.; et al. Enhanced nitrogen deposition over China. *Nature* **2013**, *494*, 459–462. [[CrossRef](#)] [[PubMed](#)]
13. Wu, Y.; Gu, B.; Erisman, J.W.; Reis, S.; Fang, Y.; Lu, X.; Zhang, X. PM_{2.5} pollution is substantially affected by ammonia emissions in China. *Environ. Pollut.* **2016**, *218*, 86–94. [[CrossRef](#)] [[PubMed](#)]
14. Li, L.; Kumar, M.; Zhu, C.; Zhong, J.; Francisco, J.S.; Zeng, X.C. Near-Barrierless Ammonium Bisulfate Formation via a Loop-Structure Promoted Proton-Transfer Mechanism on the Surface of Water. *J. Am. Chem. Soc.* **2016**, *138*, 1816–1819. [[CrossRef](#)] [[PubMed](#)]
15. Zhu, L.; Chen, Y.; Guo, L.; Wang, F. Estimate of dry deposition fluxes of nutrients over the East China Sea: The implication of aerosol ammonium to non-sea-salt sulfate ratio to nutrient deposition of coastal oceans. *Atmos. Environ.* **2013**, *69*, 131–138. [[CrossRef](#)]
16. Duce, R.A.; LaRoche, J.; Altieri, K.; Arrigo, K.R.; Baker, A.R.; Capone, D.G.; Cornell, S.; Dentener, F.; Galloway, J.; Ganeshram, R.S.; et al. Impacts of atmospheric anthropogenic nitrogen on the open ocean. *Science* **2008**, *320*, 893–897. [[CrossRef](#)] [[PubMed](#)]
17. Chen, H.Y.; Chen, L.D.; Chiang, Z.Y.; Hung, C.C.; Lin, F.J.; Chou, W.C.; Gong, G.C.; Wen, L.S. Size fractionation and molecular composition of water-soluble inorganic and organic nitrogen in aerosols of a coastal environment. *J. Geophys. Res.* **2010**, *115*. [[CrossRef](#)]
18. Chen, Y.X.; Chen, H.Y.; Wang, W.; Yeh, J.X.; Chou, W.C.; Gong, G.C.; Tsai, F.J.; Huang, S.J.; Lin, C.T. Dissolved organic nitrogen in wet deposition in a coastal city (Keelung) of the southern East China Sea: Origin, Molecular composition and flux. *Atmos. Environ.* **2015**, *112*, 20–31. [[CrossRef](#)]
19. Bronk, D.A.; See, J.H.; Bradley, P.; Killberg, L. DON as a source of bioavailable nitrogen for phytoplankton. *Biogeosciences* **2007**, *4*, 283–296. [[CrossRef](#)]
20. Shi, J.; Gao, H.; Qi, J.; Zhang, J.; Yao, X. Sources, compositions, and distributions of water-soluble organic nitrogen in aerosols over the China Sea. *J. Geophys. Res.* **2010**, *115*. [[CrossRef](#)]

21. Yang, J.Y.T.; Hsu, S.C.; Dai, M.H.; Hsiao, S.S.Y.; Kao, S.J. Isotopic composition of water-soluble nitrate in bulk atmospheric deposition at Dongsha Island: Sources and implications of external N supply to the northern South China Sea. *Biogeosciences* **2014**, *11*, 1833–1846. [[CrossRef](#)]
22. Kim, T.W.; Lee, K.; Duce, R.A.; Liss, P. Impact of atmospheric nitrogen deposition on phytoplankton productivity in the South China Sea. *Geophys. Res. Lett.* **2014**, *41*, 3156–3162. [[CrossRef](#)]
23. Grosse, J.; Bombar, D.; Doan, H.N.; Nguyen, L.N.; Voss, M. The Mekong River plume fuels nitrogen fixation and determines phytoplankton species distribution in the South China Sea during low and high discharge season. *Limnol. Oceanogr.* **2010**, *55*, 1668–1680. [[CrossRef](#)]
24. Liu, S.M.; Hong, G.H.; Zhang, J.; Ye, X.W.; Jiang, X.L. Nutrient budgets for large Chinese estuaries. *Biogeosciences* **2009**, *6*, 2245–2263. [[CrossRef](#)]
25. Kim, T.W.; Lee, K.; Lee, C.K.; Jeong, H.D.; Suh, Y.S.; Lim, W.A.; Kim, K.Y.; Jeong, H.J. Interannual nutrient dynamics in Korean coastal waters. *Harmful Algae* **2013**, *30*, S15–S27. [[CrossRef](#)]
26. Mace, K.A. Water-soluble organic nitrogen in Amazon Basin aerosols during the dry (biomass burning) and wet seasons. *J. Geophys. Res.* **2003**, *108*. [[CrossRef](#)]
27. Pai, S.C.; Tsau, Y.J.; Yang, T.I. pH and buffering capacity problems involved in the determination of ammonia in saline water using the indophenol blue spectrophotometric method. *Anal. Chim. Acta* **2001**, *434*, 209–216. [[CrossRef](#)]
28. Pai, S.C.; Yang, C.C. Formation kinetics of the pink azo dye in the determination of nitrite in natural waters. *Anal. Chim. Acta* **1990**, *232*, 345–349. [[CrossRef](#)]
29. Pai, S.C.; Riley, J.P. Determination of Nitrate in the Presence of Nitrite in Natural Waters by Flow Injection Analysis with a Non-Quantitative On-Line Cadmium Reductor. *Int. J. Environ. Anal. Chem.* **1994**, *57*, 263–277. [[CrossRef](#)]
30. Bronk, D.A.; Lomas, M.W.; Glibert, P.M.; Schukert, K.J.; Sanderson, M.P. Total dissolved nitrogen analysis: Comparisons between the persulfate, UV and high temperature oxidation methods. *Mar. Chem.* **2000**, *69*, 163–178. [[CrossRef](#)]
31. Chen, H.Y.; Chen, L.D. Importance of anthropogenic inputs and continental-derived dust for the distribution and flux of water-soluble nitrogen and phosphorus species in aerosol within the atmosphere over the East China Sea. *J. Geophys. Res.* **2008**, *113*. [[CrossRef](#)]
32. Chen, H.Y.; Chen, L.D. Occurrence of water soluble organic nitrogen in aerosols at a coastal area. *J. Atmos. Chem.* **2010**, *65*, 49–71. [[CrossRef](#)]
33. Libes, S.M. *Introduction to Marine Biogeochemistry*, 2nd ed.; Amsterdam Academic Press: Amsterdam, The Netherlands, 2009.
34. Wang, Y.; Zhuang, G.; Zhang, X.; Huang, K.; Xu, C.; Tang, A.; Chen, J.; An, Z. The ion chemistry, seasonal cycle, and sources of PM_{2.5} and TSP aerosol in Shanghai. *Atmos. Environ.* **2006**, *40*, 2935–2952. [[CrossRef](#)]
35. Keene, W.C.; Pszenny, A.A.P.; Galloway, J.N.; Hawley, M.E. Sea-salt corrections and interpretation of constituent ratios in marine precipitation. *J. Geophys. Res. Atmos.* **1986**, *91*, 6647–6658. [[CrossRef](#)]
36. Yeatman, S.G.; Spokes, L.J.; Jickells, T.D. Comparisons of coarse-mode aerosol nitrate and ammonium at two polluted coastal sites. *Atmos. Environ.* **2001**, *35*, 1321–1335. [[CrossRef](#)]
37. Lawrence, M.G.; Lelieveld, J. Atmospheric pollutant outflow from southern Asia: A review. *Atmos. Chem. Phys.* **2010**, *10*, 11017–11096. [[CrossRef](#)]
38. Xiao, H.W.; Xiao, H.Y.; Luo, L.; Shen, C.Y.; Long, A.M.; Chen, L.; Long, Z.H.; Li, D.N. Atmospheric aerosol compositions over the South China Sea: Temporal variability and source apportionment. *Atmos. Chem. Phys.* **2017**, *17*, 3199–3214. [[CrossRef](#)]
39. Zhang, M.; Chen, J.M.; Wang, T.; Cheng, T.T.; Lin, L.; Bhatia, R.S.; Hanvey, M. Chemical characterization of aerosols over the Atlantic Ocean and the Pacific Ocean during two cruises in 2007 and 2008. *J. Geophys. Res.* **2010**, *115*. [[CrossRef](#)]
40. Baker, A.R.; Lesworth, T.; Adams, C.; Jickells, T.D.; Ganzeveld, L. Estimation of atmospheric nutrient inputs to the Atlantic Ocean from 50° N to 50° S based on large-scale field sampling: Fixed nitrogen and dry deposition of phosphorus. *Glob. Biogeochem. Cycles* **2010**, *24*, GB3006. [[CrossRef](#)]
41. Galloway, J.N.; Dentener, F.J.; Capone, D.G.; Boyer, E.W.; Howarth, R.W.; Seitzinger, S.P.; Asner, G.P.; Cleveland, C.C.; Green, P.A.; Holland, E.A.; et al. Nitrogen Cycles: Past, Present, and Future. *Biogeochemistry* **2004**, *70*, 153–226. [[CrossRef](#)]

42. Jickells, T.D.; Kelly, S.D.; Baker, A.R.; Biswas, K.; Dennis, P.F.; Spokes, L.J.; Witt, M.; Yeatman, S.G. Isotopic evidence for a marine ammonia source. *Geophys. Res. Lett.* **2003**, *30*. [[CrossRef](#)]
43. Zhang, R.; Jing, J.; Tao, J.; Hsu, S.C.; Wang, G.; Cao, J.; Lee, C.S.L.; Zhu, L.; Chen, Z.; Zhao, Y.; et al. Chemical characterization and source apportionment of PM 2.5 in Beijing: Seasonal perspective. *Atmos. Chem. Phys.* **2013**, *13*, 7053–7074. [[CrossRef](#)]
44. Aneja, V.P.; Roelle, P.A.; Murray, G.C.; Southerland, J.; Erismann, J.W.; Fowler, D.; Asman, W.A.H.; Patni, N. Atmospheric nitrogen compounds II: Emissions, transport, transformation, deposition and assessment. *Atmos. Environ.* **2001**, *35*, 1903–1911. [[CrossRef](#)]
45. Pryor, S.C.; Sørensen, L.L. Dry deposition of reactive nitrogen to marine environments: Recent advances and remaining uncertainties. *Mar. Pollut. Bull.* **2002**, *44*, 1336–1340. [[CrossRef](#)]
46. Luo, L.; Kao, S.J.; Bao, H.; Xiao, H.; Yao, X.; Gao, H.; Li, J.; Li, Y. Sources of reactive nitrogen in marine aerosol over the Northwest Pacific Ocean in spring. *Atmos. Chem. Phys. Discuss.* **2017**, 1–30. [[CrossRef](#)]
47. Luo, L.; Yao, X.H.; Gao, H.W.; Hsu, S.C.; Li, J.W.; Kao, S.J. Nitrogen speciation in various types of aerosols in spring over the northwestern Pacific Ocean. *Atmospheric Chem. Phys.* **2016**, *16*, 325–341. [[CrossRef](#)]
48. Srinivas, B.; Sarin, M.M.; Sarma, V.V.S.S. Atmospheric dry deposition of inorganic and organic nitrogen to the Bay of Bengal: Impact of continental outflow. *Mar. Chem.* **2011**, *127*, 170–179. [[CrossRef](#)]
49. Zamora, L.M.; Prospero, J.M.; Hansell, D.A. Organic nitrogen in aerosols and precipitation at Barbados and Miami: Implications regarding sources, transport and deposition to the western subtropical North Atlantic. *J. Geophys. Res.* **2011**, 116. [[CrossRef](#)]
50. Nehir, M.; Koçak, M. Atmospheric Water-Soluble Organic Nitrogen (WSO_N) in the Eastern Mediterranean: Origin and Ramifications Regarding Marine Productivity. *Atmos. Chem. Phys. Discuss.* [[CrossRef](#)]
51. Chen, Y.; Mills, S.; Street, J.; Golan, D.; Post, A.; Jacobson, M.; Paytan, A. Estimates of atmospheric dry deposition and associated input of nutrients to Gulf of Aqaba seawater. *J. Geophys. Res.* **2007**, 112. [[CrossRef](#)]
52. Martino, M.; Hamilton, D.; Baker, A.R.; Jickells, T.D.; Bromley, T.; Nojiri, Y.; Quack, B.; Boyd, P.W. Western Pacific atmospheric nutrient deposition fluxes. their impact on surface ocean productivity. *Glob. Biogeochem. Cycles* **2014**, *28*, 712–728. [[CrossRef](#)]
53. Matsumoto, K.; Yamamoto, Y.; Nishizawa, K.; Kaneyasu, N.; Irino, T.; Yoshikawa-Inoue, H. Origin of the water-soluble organic nitrogen in the maritime aerosol. *Atmos. Environ.* **2017**, *167*, 97–103. [[CrossRef](#)]
54. Zhang, Q.; Duan, F.; He, K.; Ma, Y.; Li, H.; Kimoto, T.; Zheng, A. Organic nitrogen in PM 2.5 in Beijing. *Front. Environ. Sci. Eng.* **2015**, *9*, 1004–1014. [[CrossRef](#)]
55. Ho, K.F.; Ho, S.S.H.; Huang, R.J.; Liu, S.X.; Cao, J.J.; Zhang, T.; Chuang, H.C.; Chan, C.S.; Hu, D.; Tian, L. Characteristics of water-soluble organic nitrogen in fine particulate matter in the continental area of China. *Atmos. Environ.* **2015**, *106*, 252–261. [[CrossRef](#)]
56. Wu, Y.; Zhang, J.; Liu, S.; Jiang, Y.; Huang, X. Aerosol concentrations and atmospheric dry deposition fluxes of nutrients over Daya Bay. South China Sea. *Mar. Pollut. Bull.* **2018**, *128*, 106–114. [[CrossRef](#)] [[PubMed](#)]
57. Yu, X.; Yu, Q.; Zhu, M.; Tang, M.; Li, S.; Yang, W.; Zhang, Y.; Deng, W.; Li, G.; Yu, Y.; et al. Water Soluble Organic Nitrogen (WSO_N) in Ambient Fine Particles Over a Megacity in South China: Spatiotemporal Variations and Source Apportionment. *J. Geophys. Res. Atmos.* **2017**, *122*, 13045–13060. [[CrossRef](#)]
58. Karthikeyan, S.; He, J.; Palani, S.; Balasubramanian, R.; Burger, D. Determination of total nitrogen in atmospheric wet and dry deposition samples. *Talanta* **2009**, *77*, 979–984. [[CrossRef](#)] [[PubMed](#)]
59. Kang, C.H.; Kim, W.H.; Ko, H.J.; Hong, S.B. Asian Dust effects on Total Suspended Particulate (TSP) compositions at Gosan in Jeju Island. Korea. *Atmos. Res.* **2009**, *94*, 345–355. [[CrossRef](#)]
60. Jickells, T.; Baker, A.R.; Cape, J.N.; Cornell, S.E.; Nemitz, E. The cycling of organic nitrogen through the atmosphere. *Philos. Trans. R. Soc. Lond. B Biol. Sci.* **2013**, *368*, 20130115. [[CrossRef](#)] [[PubMed](#)]
61. Kanakidou, M.; Duce, R.A.; Prospero, J.M.; Baker, A.R.; Benitez-Nelson, C.; Dentener, F.J.; Hunter, K.A.; Liss, P.S.; Mahowald, N.; Okin, G.S.; et al. Atmospheric fluxes of organic N and P to the global ocean. *Glob. Biogeochem. Cycles* **2012**, *26*. [[CrossRef](#)]
62. Hoppel, W.A. Surface source function for sea-salt aerosol and aerosol dry deposition to the ocean surface. *J. Geophys. Res.* **2002**, 107. [[CrossRef](#)]
63. Hsu, C.A.; Lee, C.S.L.; Huh, C.A.; Shaheen, R.; Lin, F.J.; Liu, S.C.; Liang, M.C.; Tao, J. Ammonium deficiency caused by heterogeneous reactions during a super Asian dust episode. *J. Geophys. Res.* **2014**, 119. [[CrossRef](#)]

64. Duce, R.A.; Galloway, J.N.; Liss, P.S. The impacts of atmospheric deposition to the ocean on marine ecosystems and climate. *WMO Bull.* **2009**, *58*, 61–66.
65. Nakamura, T.; Matsumoto, K.; Uematsu, M. Chemical characteristics of aerosols transported from Asia to the East China Sea: An evaluation of anthropogenic combined nitrogen deposition in autumn. *Atmos. Environ.* **2005**. [[CrossRef](#)]
66. Jung, J.; Furutani, H.; Uematsu, M.; Kim, S.; Yoon, S. Atmospheric inorganic nitrogen input via dry, wet, and sea fog deposition to the subarctic western North Pacific Ocean. *Atmos. Chem. Phys.* **2013**, *13*, 411–428. [[CrossRef](#)]
67. Lesworth, T.; Baker, A.R.; Jickells, T. Aerosol organic nitrogen over the remote Atlantic Ocean. *Atmos. Environ.* **2010**, *44*, 1887–1893. [[CrossRef](#)]
68. Srinivas, B.; Sarin, M.M. Atmospheric deposition of N, P and Fe to the Northern Indian Ocean: Implications to C- and N-fixation. *Sci. Total Environ.* [[CrossRef](#)]
69. Jung, J.; Furutani, H.; Uematsu, M. Atmospheric inorganic nitrogen in marine aerosol and precipitation and its deposition to the North and South Pacific Oceans. *J. Atmos. Chem.* **2011**, *68*, 157–181. [[CrossRef](#)]
70. Wang, X.; Wu, Z.; Shao, M.; Fang, Y.; Zhang, L.; Chen, F.; Chan, P.-w.; Fan, Q.; Wang, Q.; Zhu, S.; et al. Atmospheric nitrogen deposition to forest and estuary environments in the Pearl River Delta region, southern China. *Tellus B Chem. Phys. Meteorol.* **2013**, *65*, 20480. [[CrossRef](#)]
71. Shih, Y.Y.; Hung, C.C.; Gong, G.C.; Chung, W.C.; Wang, Y.H.; Lee, I.H.; Chen, K.S.; Ho, C.Y. Enhanced Particulate Organic Carbon Export at Eddy Edges in the Oligotrophic Western North Pacific Ocean. *PLoS ONE* **2015**, *10*, e0131538. [[CrossRef](#)] [[PubMed](#)]
72. Hung, C.C.; Gong, G. CPOC/234Th ratios in particles collected in sediment traps in the northern South China Sea. *Estuar. Coast. Shelf Sci.* **2010**, *88*, 303–310. [[CrossRef](#)]
73. Yan, G.; Kim, G. Sources and fluxes of organic nitrogen in precipitation over the southern East Sea/Sea of Japan. *Atmos. Chem. Phys.* **2015**, *15*, 2761–2774. [[CrossRef](#)]
74. Li, D.; Chou, W.C.; Shih, Y.Y.; Chen, G.Y.; Chang, Y.; Chow, C.H.; Lin, T.Y.; Hung, C.C. Elevated particulate organic carbon export flux induced by internal waves in the oligotrophic northern South China Sea. *Sci. Rep.* **2018**, *8*, 2042. [[CrossRef](#)] [[PubMed](#)]
75. Sandroni, V.; Raimbault, P.; Migon, C.; Raimbault, P.; Migon, C.; Garcia, N.; Gouze, E. Dry atmospheric deposition and diazotrophy as sources of new nitrogen to northwestern Mediterranean oligotrophic surface waters. *Deep Sea Res. Part I Oceanogr. Res. Pap.* **2007**, *54*, 1859–1870. [[CrossRef](#)]



© 2018 by the authors. Licensee MDPI, Basel, Switzerland. This article is an open access article distributed under the terms and conditions of the Creative Commons Attribution (CC BY) license (<http://creativecommons.org/licenses/by/4.0/>).